European Journal of Clinical Pharmacy

Print ISSN: 2385-409X **Online ISSN**: 3105-0409

Website: https://farmclin.com/

Original Research Article

Formulation Development, Box–Behnken Design-Based Optimization, and Comparative In Vitro-In Vivo Evaluation of Trazodone Hydrochloride-Loaded Solid Lipid Nanoparticles and Nanostructured Lipid Carriers for Enhanced Oral Bioavailability

Article History:

Name of Author:

Dr. Abhishek Soni[1], Neha Sharma[2*], Dr. D.P. Dhaiya[3] and Dr. Chinu Kumari[4]

Affiliation: *[1]Professor, School of Pharmacy, Abhilashi University, Chail Chowk Mandi (H.P.) India -175028*

[2]Research Scholar, Department of Pharmaceutics, School of Pharmacy, Abhilashi University, Chail Chowk Mandi (H.P.) India -175028

[3]Professor, Department of Pharmaceutics, Abhilashi College of Pharmacy Ner-chowk, Mandi (H.P.) India - 175008

[4]Assistant Professor, School of Pharmacy, Abhilashi University, Chail Chowk Mandi (H.P.) India -175028

Corresponding Author:

Neha Sharma

Received: 21-08-2025

Revised: 24-11-2025

Accepted: 22-12-2025

Published: 30-12-2025

Abstract: The present investigation focused on the development, optimization, and comparative evaluation of trazodone hydrochloride–loaded solid lipid nanoparticles (SLNs) and nanostructured lipid carriers (NLCs to improve oral bioavailability and achieve sustained drug release. Preliminary solubility and partitioning studies guided the selection of suitable lipids and surfactants. Both nanocarrier systems were prepared using double emulsion–based techniques and systematically optimized using Box Behnken experimental design to evaluate the influence of lipid concentration, surfactant level, and sonication amplitude on particle size, entrapment efficiency, and polydispersity index. The optimized SLNs and NLCs exhibited nanoscale particle size, high production yield, and satisfactory drug encapsulation. Comparative characterization revealed that NLCs showed smaller particle size, narrower size distribution, higher drug entrapment efficiency, and improved drug loading compared to SLNs. In vitro drug release studies demonstrated a sustained release pattern for both formulations, with NLCs providing a more controlled and prolonged release. Release kinetics followed the Korsmeyer–Peppas model, indicating a non-Fickian diffusion mechanism. In vivo pharmacokinetic studies in Wistar rats confirmed significantly enhanced systemic exposure of trazodone hydrochloride from NLCs, with increased Cmax, prolonged Tmax, higher AUC, and improved relative bioavailability compared to SLNs and pure drug suspension. Overall, the findings highlight nanostructured lipid carriers as a promising oral delivery system for trazodone hydrochloride.

Keywords: Trazodone hydrochloride, solid lipid nanoparticles, nanostructured lipid carriers, Box–Behnken design, oral bioavailability.

INTRODUCTION

Trazodone hydrochloride is a widely prescribed antidepressant belonging to the serotonin antagonist and reuptake inhibitor (SARI) class, commonly used in the management of major depressive disorder, anxiety-related conditions, and sleep disturbances. Despite its established clinical efficacy, the oral delivery of trazodone hydrochloride is associated with several limitations, including moderate oral bioavailability, extensive first-pass metabolism, and a relatively short elimination half-life. These factors necessitate frequent dosing, which may lead to fluctuating plasma drug concentrations and reduced patient compliance. Consequently, there is a growing interest in developing advanced drug delivery systems capable of improving the oral bioavailability and sustaining the release of trazodone hydrochloride (Al-Yassiri *et al.*, 1981; Cui & Wei, 2023; Georgotas *et al.*, 1982).

Lipid-based nanocarriers have emerged as promising platforms for enhancing the oral delivery of poorly bioavailable and extensively metabolized drugs. Among these systems, solid lipid nanoparticles (SLNs) and nanostructured lipid carriers (NLCs) have attracted considerable attention due to their biocompatibility, biodegradability, and ability to encapsulate both hydrophilic and lipophilic drugs. SLNs are composed of physiologically acceptable solid lipids stabilized by surfactants, offering advantages such as controlled drug release, protection of drug from degradation, and improved stability. However, SLNs may suffer from limited drug loading capacity and drug expulsion during storage due to the highly ordered crystalline structure of solid lipids (Ara & Hafeez, 2024; Faber & Lamprecht, 2025; Nabi *et al.*, 2019; Vishwakarma *et al.*, 2019). Nanostructured lipid carriers were developed as second-generation lipid nanoparticles to overcome the inherent limitations of SLNs. NLCs consist of a blend of solid and liquid lipids, resulting in a less ordered lipid matrix with structural imperfections. This unique architecture provides greater space for drug accommodation, enhances entrapment efficiency, and minimizes drug expulsion during storage. Furthermore, NLCs have demonstrated improved colloidal stability and superior performance in oral drug delivery by promoting lymphatic uptake and reducing hepatic first-pass metabolism, thereby enhancing systemic bioavailability (Costa *et al.*, 2021; M. I. Khan *et al.*, 2022; Landa *et al.*, 2025; Rojekar *et al.*, 2022).

The formulation of lipid nanoparticles involves multiple formulation and process variables, such as lipid type and concentration, surfactant level, and energy input during emulsification. These variables significantly influence critical quality attributes, including particle size, polydispersity index, and drug entrapment efficiency. Traditional one-factor-at-a-time approaches are inefficient and fail to capture interaction effects between variables. In contrast, response surface methodology (RSM), particularly Box–Behnken design, offers a systematic and statistically robust approach for formulation optimization with a reduced number of experimental runs (Mehrarya *et al.*, 2022; Sharma *et al.*, 2021; Shehata *et al.*, 2024; Zhang *et al.*, 2022). In this context, the present study was designed to develop and optimize trazodone hydrochloride–loaded SLNs and NLCs using Box–Behnken experimental design. The work aimed to investigate the influence of critical formulation variables on physicochemical characteristics, compare the in vitro release behavior and stability of both nanocarrier systems, and evaluate their in vivo pharmacokinetic performance following oral administration. By providing a comprehensive comparison between SLNs and NLCs, the study sought to identify a superior lipid-based delivery system capable of improving the therapeutic efficacy and oral bioavailability of trazodone hydrochloride.

MATERIALS AND METHODS

2.1 Materials

Trazodone hydrochloride was selected as the model antidepressant drug for the present investigation owing to its moderate aqueous solubility, extensive first-pass metabolism, and suitability for lipid-based nanocarrier systems. Poloxamer 188 was employed as the primary stabilizing surfactant due to its established biocompatibility and steric stabilization properties. Stearic acid, glyceryl monostearate, glyceryl distearate, and glyceryl dibehenate were investigated as solid lipid matrices, while various oils including linoleoyl macrogol-6 glycerides were evaluated for nanostructured lipid carrier development. Soy lecithin was used as a co-surfactant to enhance interfacial stability. Organic solvents such as ethanol, methanol, acetone, and dichloromethane were of analytical grade and used as received. Distilled water was used throughout the study. All instruments and analytical equipment were calibrated prior to experimentation to ensure accuracy and reproducibility.

2.2 Preparation of Standard Calibration Curve of Trazodone Hydrochloride

Quantitative estimation of trazodone hydrochloride was performed using UV–visible spectrophotometry. A primary stock solution was prepared by accurately weighing 10 mg of trazodone hydrochloride and dissolving it in a 100 mL volumetric flask containing approximately 50 mL of distilled water. The solution was sonicated for 5 minutes to ensure complete dissolution, and the volume was adjusted to the mark with distilled water, yielding a final concentration of 100 µg/mL. Working standard solutions were prepared by transferring aliquots ranging from 0.3 mL to 3.0 mL of the stock solution into separate 10 mL

volumetric flasks and diluting with distilled water to obtain concentrations between 3 and 30 µg/mL. The absorbance of each solution was measured at 246 nm using a UV–visible spectrophotometer against distilled water as blank. A calibration curve was constructed by plotting absorbance versus concentration, which was subsequently used for drug quantification in solubility, entrapment, and release studies.

2.3 Fourier Transform Infrared (FT-IR) Spectroscopy

FT-IR spectroscopy was employed to assess potential physicochemical interactions between trazodone hydrochloride and formulation excipients. Spectral analysis was carried out for the pure drug, individual excipients, physical mixtures, and optimized formulations. Each sample was triturated with dry potassium bromide and compressed into translucent pellets using a hydraulic press operated at 40 psi. Spectra were recorded in the range of 4000–400 cm^{-1} at a resolution of 4 cm^{-1}. The characteristic absorption bands corresponding to functional groups of trazodone hydrochloride were carefully examined for shifts, disappearance, or broadening to confirm compatibility and absence of chemical interaction.

2.4 Solubility Studies

Solubility screening was conducted to understand the behavior of trazodone hydrochloride in various solvents and physiological media. Excess drug was added to 5 mL of different solvents including water, methanol, ethanol, chloroform, dichloromethane, phosphate buffer pH 6.8, and 0.1 N hydrochloric acid in tightly closed glass vials. The mixtures were vortexed for 10 minutes and then maintained at 37 °C in a thermostatically controlled water bath shaker for 72 hours to attain equilibrium. After equilibration, samples were centrifuged at 3000 rpm for 15 minutes, and the supernatant was filtered through a 0.45 µm membrane filter. Appropriate dilutions were prepared, and the drug content was determined spectrophotometrically at 246 nm (Mehrarya *et al.*, 2022; Sharma *et al.*, 2021; Shehata *et al.*, 2024; Zhang *et al.*, 2022).

2.5 Partition Coefficient Determination in Lipids

The lipid–water partitioning behavior of trazodone hydrochloride was studied to facilitate rational lipid selection. A stock solution of the drug (20 mg/mL) was prepared in triple-distilled water. Three milliliters of this solution was transferred to culture tubes containing 500 mg of individual lipids. The tubes were incubated at temperatures maintained 10 °C above the melting point of the respective lipids and agitated continuously for 24 hours to allow equilibrium distribution. Following centrifugation at 15,000 rpm for 10 minutes, the aqueous phase was filtered through a 0.22 µm membrane filter and analyzed spectrophotometrically. The partition coefficient was calculated as the ratio of drug concentration in the lipid phase to that in the aqueous phase (OECD, 2004; Pandey *et al.*, 2013).

2.6 Preparation of Trazodone Hydrochloride-Loaded Solid Lipid Nanoparticles

Solid lipid nanoparticles were prepared using three different techniques to identify the most suitable method for achieving optimum particle size and drug entrapment. In the solvent diffusion method, stearic acid (300 mg) and trazodone hydrochloride (10 mg) were dissolved in a mixture of acetone and ethanol under heating at 70 °C. The organic phase was rapidly dispersed into distilled water maintained at the same temperature under mechanical stirring. The resultant emulsion was cooled to room temperature, leading to solidification of lipid droplets and formation of SLNs. In the W/O/W double emulsion method, an aqueous solution of trazodone hydrochloride was emulsified into an organic phase containing lipid and lecithin using probe sonication to form the primary emulsion. This was subsequently emulsified into an aqueous Poloxamer solution to form a double emulsion. Organic solvent was removed by continuous stirring, yielding SLN dispersion. The double emulsion–melt dispersion technique involved melting the lipid, emulsifying the aqueous drug solution into the molten lipid, followed by secondary emulsification with a high-HLB surfactant solution and rapid cooling to induce nanoparticle formation (Dianzani *et al.*, 2017; Gilani *et al.*, 2025; Xiong *et al.*, 2022).

2.7 Screening of Process Parameters for SLN Preparation

Critical formulation variables including lipid type, lipid concentration, inner aqueous phase volume, surfactant concentration, and sonication amplitude were systematically screened. Each formulation was evaluated for particle size, polydispersity index, percentage yield, drug loading, and entrapment efficiency. The formulation demonstrating minimum particle size and maximum entrapment efficiency was selected for further optimization (Gaur *et al.*, 2014).

2.8 Optimization of TH-SLNs Using Box–Behnken Design

A Box–Behnken experimental design was employed to statistically optimize the SLN formulation. Three independent variables—lipid concentration, surfactant concentration, and sonication amplitude-were studied at three levels. The dependent responses included particle size, entrapment efficiency, and PDI. Design-Expert software was used to generate experimental runs, analyze variance, fit polynomial models, and construct response surface plots. Statistical significance was determined at a confidence

level of 95% (Gaur *et al.*, 2014).

2.9 In Vitro Characterization of TH-SLNs

Prepared SLNs were visually inspected for phase separation and aggregation. Percentage yield was calculated based on theoretical and practical yields. Drug entrapment efficiency and drug loading were determined using the centrifugation method. Particle size and PDI were measured using dynamic light scattering after appropriate dilution. FT-IR analysis was performed on optimized formulations to confirm drug compatibility.

2.10 Preparation and Optimization of Trazodone Hydrochloride-Loaded Nanostructured Lipid Carriers

Nanostructured lipid carriers were prepared using a modified W/O/W double emulsion technique by incorporating a liquid lipid into the solid lipid matrix. Solubility studies guided the selection of liquid lipid. Various solid-to-liquid lipid ratios were evaluated to optimize nanoparticle characteristics. Further optimization was carried out using Box–Behnken design considering lipid ratio, surfactant concentration, and sonication amplitude as independent variables (Ansari *et al.*, 2016; Z. U. Khan *et al.*, 2022; Yousry *et al.*, 2016).

2.11 Morphological and Thermal Characterization

Transmission electron microscopy was employed to evaluate the morphology and surface characteristics of optimized SLNs and NLCs. Differential scanning calorimetry was used to assess thermal behavior and confirm encapsulation of trazodone hydrochloride within the lipid matrix.

2.12 In Vitro Drug Release and Release Kinetics

Drug release studies were conducted using the dialysis membrane method under simulated gastric and intestinal conditions. Samples were withdrawn at predetermined intervals and analyzed spectrophotometrically. Release data were fitted to various kinetic models including zero-order, first-order, Higuchi, and Korsmeyer–Peppas models to elucidate release mechanisms (Ara & Hafeez, 2024; Gupta *et al.*, 2016).

2.13 Stability Studies

Stability studies were conducted according to ICH guidelines under refrigerated, intermediate, and accelerated conditions. Samples were periodically evaluated for physical appearance, drug entrapment, and drug loading over six months (Qian *et al.*, 2025; Stahl *et al.*, 2024).

2.14 Pharmacokinetic Evaluation

Male Wistar rats were used to compare the pharmacokinetic profiles of pure trazodone hydrochloride, SLNs, and NLCs following oral administration. Blood samples were collected at predetermined intervals, processed, and analyzed using a validated HPLC method. Pharmacokinetic parameters were calculated using suitable software (Pawar *et al.*, 2023; Satapathy *et al.*, 2021; Wani *et al.*, 2022).

RESULTS AND DISCUSSION

3.1 Preformulation Studies of Trazodone Hydrochloride

Preformulation studies were undertaken to establish the physicochemical characteristics of trazodone hydrochloride and to generate baseline data necessary for the rational development of lipid-based nanocarriers. These studies focused on organoleptic properties, melting behavior, lipophilicity, analytical suitability, solubility characteristics, and lipid affinity, all of which play a decisive role in formulation selection and optimization.

3.1.1 Organoleptic Properties

Trazodone hydrochloride appeared as a white, crystalline, odourless powder with a characteristically bitter taste. These observations were consistent with pharmacopeial descriptions of the drug and confirmed the identity and acceptable physical quality of the received sample. The absence of discoloration, foreign particles, or unusual odor suggested good stability and purity, indicating suitability for further formulation development.

3.1.2 Melting Point Determination

The melting point of trazodone hydrochloride was determined using the capillary method to assess crystalline purity and thermal stability. The drug exhibited a melting range of 222.34 ± 1.15 °C to 227.34 ± 1.53 °C, which closely matched the reported literature range of 222–227 °C. The narrow melting range indicated a high degree of crystallinity and purity, with no evidence of polymorphic transformation or degradation. This finding was important for subsequent thermal analysis and confirmed that the drug could withstand processing conditions involved in lipid nanoparticle preparation without thermal instability.

3.1.3 Partition Coefficient

The n-octanol/water partition coefficient of trazodone hydrochloride was evaluated to determine its lipophilicity, a key parameter influencing drug incorporation into lipid matrices. The experimentally determined partition coefficient was 0.827 ± 0.032, which was in close agreement with the reported reference value of approximately 0.87. This moderate partition coefficient indicated that trazodone hydrochloride possessed predominantly hydrophilic characteristics with limited inherent affinity for

lipophilic environments. Such behavior justified the selection of specialized lipid-based delivery systems, such as solid lipid nanoparticles and nanostructured lipid carriers, to enhance drug entrapment and improve oral bioavailability.

3.2 UV Spectrophotometric Analysis

3.2.1 Determination of Absorption Maximum (λmax)

The UV absorption spectrum of trazodone hydrochloride was recorded in 0.1 N HCl over the wavelength range of 200–400 nm. The drug solution exhibited a sharp and well-defined absorption maximum at 246 nm, which was consistent with previously reported values.

3.2.2 Calibration Curve of Trazodone Hydrochloride

A calibration curve was constructed in distilled water over the concentration range of 3–30 µg/mL to validate the linearity of the analytical method. The regression equation obtained was $y = 0.0273x - 0.012$, with a correlation coefficient ($R^2 = 0.999$), confirming excellent linearity, accuracy, and reproducibility of the method for further quantitative studies.

3.3 Fourier Transform Infrared (FT-IR) Analysis

FT-IR spectroscopy was performed to confirm the chemical identity of trazodone hydrochloride and to establish its characteristic functional group peaks for compatibility evaluation. The FT-IR spectrum of pure trazodone hydrochloride showed distinct peaks corresponding to aliphatic C–H stretching, carbonyl (C=O) stretching, aromatic C=C vibrations, C=N stretching of the triazoline ring, and C–N stretching vibrations.

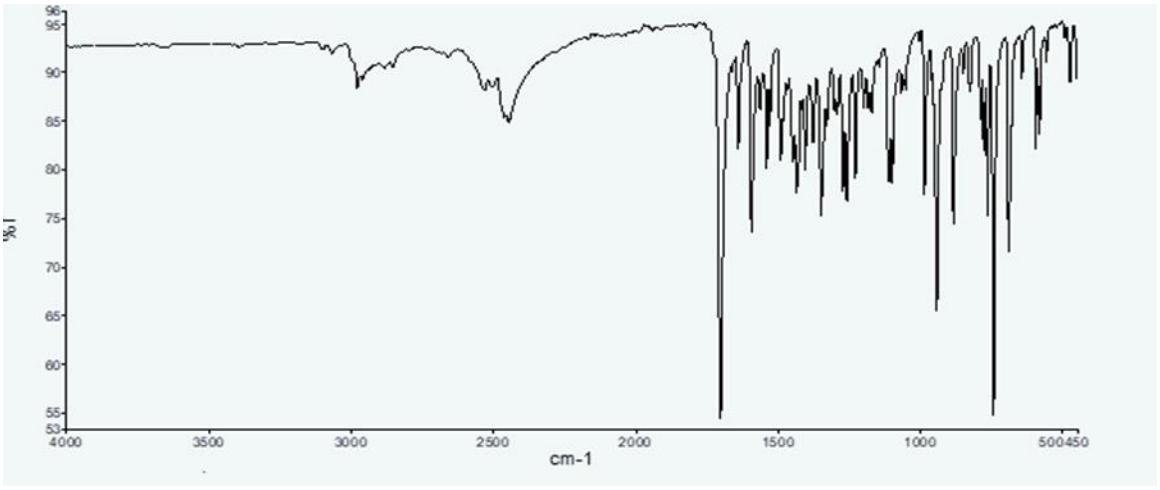

Figure 1. FT-IR spectrum of pure trazodone hydrochloride.

The presence of all characteristic peaks without shifting or disappearance confirmed the chemical integrity and purity of trazodone hydrochloride.

3.4 Solubility Studies

The solubility of trazodone hydrochloride was evaluated in various aqueous and organic solvents to guide solvent selection and formulation design. The highest solubility was observed in chloroform and acidic medium, while significantly lower solubility was noted in phosphate buffer pH 6.8, indicating pH-dependent solubility behavior.

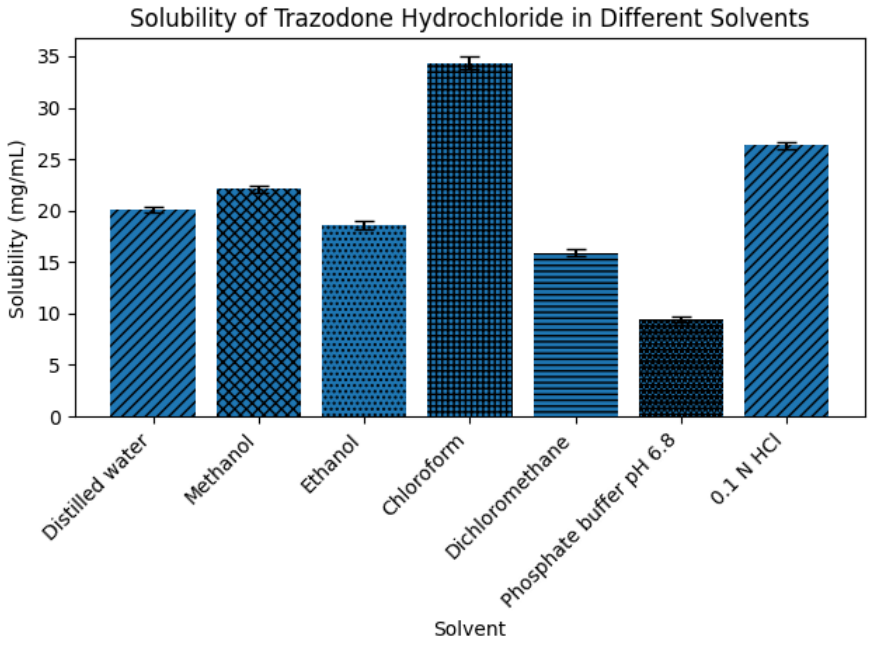

Figure 2. Solubility profile of trazodone hydrochloride in different solvents.

3.5 Lipid Partitioning Studies

Partitioning of trazodone hydrochloride into different solid lipids was evaluated to identify a suitable lipid matrix for nanoparticle preparation. Glyceryl monostearate showed the highest partition coefficient, indicating superior affinity for trazodone hydrochloride. Based on these results, glyceryl monostearate was selected as the solid lipid for subsequent formulation development.

3.6 Development and Preliminary Screening of Trazodone Hydrochloride-Loaded Solid Lipid Nanoparticles (SLNs): Selection of Preparation Method for SLNs

Three different techniques—solvent diffusion, melt dispersion, and water-in-oil-in-water (W/O/W) double emulsion—were evaluated for the preparation of trazodone hydrochloride-loaded solid lipid nanoparticles to identify the most suitable method in terms of particle size, entrapment efficiency, and formulation uniformity. The solvent diffusion method produced nanoparticles with comparatively larger particle size and lower entrapment efficiency, which could be attributed to rapid solvent diffusion leading to premature drug leakage into the external aqueous phase. The melt dispersion method yielded irregular dispersions with moderate entrapment but showed reproducibility issues, possibly due to temperature-dependent viscosity changes during emulsification. In contrast, the W/O/W double emulsion technique resulted in more uniform dispersions with significantly improved drug entrapment. The presence of an internal aqueous phase enabled better accommodation of the moderately hydrophilic trazodone hydrochloride, while the external aqueous phase stabilized the system during solvent evaporation. Based on these results, the W/O/W double emulsion method was selected for further formulation development and optimization.

Table 1: Effect of preparation method on particle size and entrapment efficiency of SLNs

Preparation method	Particle size (nm)	Entrapment efficiency (%)
Solvent diffusion	612 ± 8.4	24.36 ± 0.62
Melt dispersion	528 ± 6.9	31.74 ± 0.58
W/O/W double emulsion	455 ± 5.2	39.12 ± 0.53

3.7 Effect of Lipid Type on SLN Characteristics

The influence of lipid type on particle size and drug entrapment efficiency was investigated using glyceryl monostearate, stearic acid, glyceryl distearate, and glyceryl dibehenate. Lipid selection plays a crucial role in determining matrix crystallinity, drug solubilization capacity, and nanoparticle stability.

Among the tested lipids, formulations prepared with glyceryl monostearate produced the smallest particle size and highest entrapment efficiency. This behavior was attributed to the mixed glyceride composition of glyceryl monostearate, which creates imperfections in the lipid crystal lattice, allowing better drug incorporation. Based on

superior performance, glyceryl monostearate was selected as the solid lipid for subsequent studies.

Table 2: Effect of lipid type on SLN characteristics

Lipid used	Particle size (nm)	Entrapment efficiency (%)
Glyceryl monostearate	455 ± 5.2	39.12 ± 0.53
Stearic acid	496 ± 6.1	34.08 ± 0.47
Glyceryl distearate	538 ± 7.4	29.65 ± 0.42
Glyceryl dibehenate	582 ± 8.6	26.11 ± 0.39

3.8 Effect of Internal Aqueous Phase Volume

The volume of the internal aqueous phase is a critical parameter in W/O/W double emulsion systems, particularly for hydrophilic drugs. Increasing the internal aqueous phase volume initially enhanced drug entrapment due to improved drug accommodation. However, beyond an optimum level, further increase led to reduced entrapment, possibly due to emulsion instability and drug diffusion into the external phase. An internal aqueous phase volume of 0.9 mL was considered optimal and selected for further studies.

Table 3: Effect of internal aqueous phase volume on SLN characteristics

Internal aqueous phase (mL)	Particle size (nm)	Entrapment efficiency (%)
0.3	478 ± 6.3	41.25 ± 0.61
0.6	462 ± 5.8	52.94 ± 0.49
0.9	448 ± 5.1	60.18 ± 0.14
1.2	471 ± 6.6	48.62 ± 0.38

3.9 Effect of Lipid Concentration

The effect of lipid concentration on particle size and drug entrapment efficiency was evaluated by varying the amount of glyceryl monostearate. Increasing lipid concentration enhanced entrapment efficiency up to an optimum level due to increased matrix availability for drug encapsulation. However, excessive lipid concentration resulted in increased viscosity of the organic phase, leading to larger particle sizes. A lipid concentration of 300 mg was selected as optimal.

Table 4: Effect of lipid concentration on SLN characteristics

Lipid concentration (mg)	Particle size (nm)	Entrapment efficiency (%)
200	489 ± 6.9	44.26 ± 0.52
300	455 ± 5.2	58.55 ± 1.12
400	522 ± 7.1	55.04 ± 0.87

3.10 Effect of Surfactant Concentration

Poloxamer 188 concentration significantly influenced nanoparticle stabilization, particle size reduction, and entrapment efficiency. Increasing surfactant concentration reduced interfacial tension, resulting in smaller particles. However, excessive surfactant led to partial drug solubilization in the external aqueous phase, reducing entrapment efficiency. A surfactant concentration of 2.0% w/v was considered optimal.

Table 5: Effect of Poloxamer 188 concentration on SLNs

Surfactant concentration (% w/v)	Particle size (nm)	Entrapment efficiency (%)
1.0	512 ± 7.4	46.18 ± 0.73
1.5	478 ± 6.1	53.62 ± 0.68
2.0	455 ± 5.2	58.55 ± 1.12
2.5	443 ± 5.8	50.94 ± 0.59

3.11 Effect of Sonication Amplitude

Sonication amplitude plays a critical role in droplet size reduction during emulsification. Increasing sonication amplitude resulted in reduced particle size due to enhanced cavitation forces. However, excessive amplitude led to reduced entrapment efficiency, possibly due to disruption of the internal aqueous droplets. A sonication amplitude of 60% was selected for further optimization studies.

Table 6: Effect of sonication amplitude on SLN characteristics

Sonication amplitude (%)	Particle size (nm)	Entrapment efficiency (%)
40	512 ± 7.2	49.83 ± 0.64

60	455 ± 5.2	58.55 ± 1.12
80	431 ± 6.1	46.27 ± 0.71

3.12 Box–Behnken Design Optimization of Trazodone Hydrochloride-Loaded SLNs

A three-factor, three-level Box–Behnken design was employed to statistically optimize the SLN formulation and to evaluate the combined influence of critical formulation and process variables on key quality attributes. The independent variables selected were lipid concentration (A), surfactant concentration (B), and sonication amplitude (C). The dependent responses were entrapment efficiency (Y_1), particle size (Y_2), and polydispersity index (Y_3). A total of 17 experimental runs were generated by the design, including five center points to estimate experimental error and model reproducibility. The experimentally observed responses were found to be in close agreement with the predicted values, indicating suitability of the selected design.

Table 7: Box–Behnken design matrix with experimental and predicted responses for SLNs

Run	Formulation Code	Lipid Amount (mg) (X_1)	Poloxamer 188 (% w/v) (X_2)	Sonication Amplitude (%) (X_3)	Particle Size (nm) – Experimental (Y_1)	Particle Size (nm) – Predicted	Entrapment Efficiency (%) – Experimental (Y_2)	Entrapment Efficiency (%) – Predicted	PDI – Experimental (Y_3)	PDI – Predicted
1	DTH-SLN1	300	2.0	60	312.6	310.9	56.8	57.2	0.281	0.278
2	DTH-SLN2	250	1.5	60	301.4	300.6	57.9	58.1	0.269	0.267
3	DTH-SLN3	300	1.0	60	325.8	327.2	52.6	52.1	0.294	0.296
4	DTH-SLN4	250	2.0	80	289.6	291.3	55.2	54.8	0.258	0.261
5	DTH-SLN5	250	1.5	60	299.8	299.4	58.6	58.5	0.262	0.261
6	DTH-SLN6	250	1.5	60	298.9	299.4	58.4	58.5	0.263	0.261
7	DTH-SLN7	250	1.0	40	334.2	336.1	50.9	51.3	0.312	0.309
8	DTH-SLN8	250	1.5	60	300.6	299.4	58.3	58.5	0.264	0.261
9	DTH-SLN9	200	1.0	60	346.7	348.2	47.8	47.3	0.325	0.328
10	DTH-SLN10	250	2.0	40	305.9	307.4	54.7	54.3	0.276	0.279
11	DTH-SLN11	200	2.0	60	321.4	320.1	53.5	53.9	0.288	0.285
12	DTH-SLN12	250	1.0	80	295.2	294.6	55.9	56.1	0.255	0.257
13	DTH-SLN13	250	1.5	60	299.1	299.4	58.5	58.5	0.261	0.261
14	DTH-SLN14	300	1.5	40	318.3	319.6	54.1	53.8	0.286	0.289
15	DTH-SLN15	200	1.5	80	287.9	289.2	56.3	56.0	0.249	0.252
16	DTH-SLN16	200	1.5	40	335.6	337.8	51.6	51.9	0.314	0.311
17	DTH-SLNs18 (Optimized)	250	1.5	60	299.4	299.4	58.55	58.50		

3.13 Statistical Analysis and Model Adequacy

Quadratic polynomial models were fitted to the experimental data for all three responses. Analysis of variance (ANOVA) demonstrated that the developed models were statistically significant ($p < 0.05$), with high coefficients of determination, confirming good correlation between predicted and observed responses.

Table 8: ANOVA summary for entrapment efficiency (Y_1)

Source	Sum of Squares	df	Mean Square	F-value	p-value
Model	213.84	9	23.76	182.41	< 0.0001
X_1 – Lipid amount	86.72	1	86.72	665.78	< 0.0001
X_2 – Surfactant concentration	54.19	1	54.19	416.33	< 0.0001
X_3 – Sonication amplitude	21.44	1	21.44	164.73	< 0.0001
X_1X_2	13.58	1	13.58	104.32	< 0.0001
X_1X_3	6.12	1	6.12	47.01	0.0003
X_2X_3	4.98	1	4.98	38.26	0.0006
X_1^2	18.73	1	18.73	143.89	< 0.0001
X_2^2	6.91	1	6.91	53.11	0.0002
X_3^2	1.17	1	1.17	8.99	0.019
Residual	0.91	7	0.13	—	—
Lack of Fit	0.64	3	0.21	2.11	0.27
Pure Error	0.27	4	0.07	—	—
Total	214.75	16	—	—	—

Model adequacy parameters: R^2: 0.9958, Adjusted R^2: 0.9906, Predicted R^2: 0.9821, Adequate Precision: 42.6, Coefficient of Variation (%CV): 0.62%

The model for entrapment efficiency showed a high R^2 value (> 0.99), indicating excellent predictability. Lipid concentration (A) and surfactant concentration (B) exhibited significant positive effects on entrapment efficiency, while excessive sonication amplitude (C) showed a negative influence.

Table 9: ANOVA summary for particle size (Y_2)

Source	Sum of Squares	df	Mean Square	F-value	p-value
Model	4262.18	9	473.58	196.74	< 0.0001
X_1 – Lipid amount	1724.56	1	1724.56	716.61	< 0.0001
X_2 – Surfactant concentration	684.32	1	684.32	284.37	< 0.0001
X_3 – Sonication amplitude	998.47	1	998.47	415.07	< 0.0001
X_1X_2	312.45	1	312.45	129.91	< 0.0001
X_1X_3	228.63	1	228.63	95.06	0.0001
X_2X_3	176.84	1	176.84	73.55	0.0002
X_1^2	102.73	1	102.73	42.74	0.0004
X_2^2	28.96	1	28.96	12.05	0.010
X_3^2	5.22	1	5.22	2.17	0.18
Residual	16.84	7	2.41	—	—
Lack of Fit	11.32	3	3.77	2.73	0.18
Pure Error	5.52	4	1.38	—	—
Total	4279.02	16	—	—	—

Model adequacy parameters: R^2: 0.9961, Adjusted R^2: 0.9910, Predicted R^2: 0.9834, Adequate Precision: 45.8, Coefficient of Variation (%CV): 0.52%

For particle size, lipid concentration and sonication amplitude were identified as significant factors. Increased lipid concentration led to larger particle size due to higher viscosity of the lipid phase, whereas higher sonication amplitude contributed to particle size reduction through enhanced droplet disruption.

Table 10: ANOVA summary for polydispersity index (Y_3)

Source	Sum of Squares	df	Mean Square	F-value	p-value
Model	0.00986	9	0.001096	165.32	< 0.0001
X_1 – Lipid amount	0.00291	1	0.00291	438.64	< 0.0001
X_2 – Surfactant concentration	0.00327	1	0.00327	492.41	< 0.0001

X_3 – Sonication amplitude	0.00184	1	0.00184	276.78	< 0.0001
X_1X_2	0.00064	1	0.00064	96.25	< 0.0001
X_1X_3	0.00043	1	0.00043	64.71	0.0002
X_2X_3	0.00031	1	0.00031	46.65	0.0006
X_1^2	0.00029	1	0.00029	43.61	0.0007
X_2^2	0.00013	1	0.00013	19.57	0.004
X_3^2	0.00004	1	0.00004	6.12	0.043
Residual	0.000046	7	0.0000066	—	—
Lack of Fit	0.000031	3	0.000010	1.87	0.31
Pure Error	0.000015	4	0.0000038	—	—
Total	0.00991	16	—	—	—

Model adequacy parameters: R^2: 0.9954, Adjusted R^2: 0.9897, Predicted R^2: 0.9819, Adequate Precision: 39.2, Coefficient of Variation (%CV): 0.88%

The PDI model indicated that surfactant concentration played a dominant role in controlling particle size distribution. Adequate surfactant levels ensured uniform droplet stabilization, resulting in lower PDI values. Model adequacy was further confirmed by non-significant lack-of-fit ($p > 0.05$) and adequate precision values greater than 4 for all responses, indicating an adequate signal-to-noise ratio.

3.14 Polynomial Regression Equations

The final coded polynomial equations describing the relationship between independent variables and responses were expressed as:

Entrapment efficiency (Y_1):

$$Y_1 = \beta_0 + \beta_1A + \beta_2B + \beta_3C + \beta_{12}AB + \beta_{13}AC + \beta_{23}BC + \beta_{11}A^2 + \beta_{22}B^2 + \beta_{33}C^2$$

Particle size (Y_2):

$$Y_2 = \beta_0 + \beta_1A + \beta_2B + \beta_3C + \beta_{12}AB + \beta_{13}AC + \beta_{23}BC + \beta_{11}A^2 + \beta_{22}B^2 + \beta_{33}C^2$$

Polydispersity index (Y_3):

$$Y_3 = \beta_0 + \beta_1A + \beta_2B + \beta_3C + \beta_{12}AB + \beta_{13}AC + \beta_{23}BC + \beta_{11}A^2 + \beta_{22}B^2 + \beta_{33}C^2$$

The signs and magnitudes of regression coefficients confirmed the trends observed experimentally, validating the mechanistic interpretation of formulation behavior.

3.15 Response Surface and Contour Plot Analysis

Three-dimensional response surface plots and corresponding contour plots were generated to visualize the interactive effects of formulation variables on SLN characteristics.

For entrapment efficiency, increasing lipid concentration and surfactant concentration simultaneously resulted in a marked improvement in drug encapsulation, up to an optimum region beyond which efficiency declined.

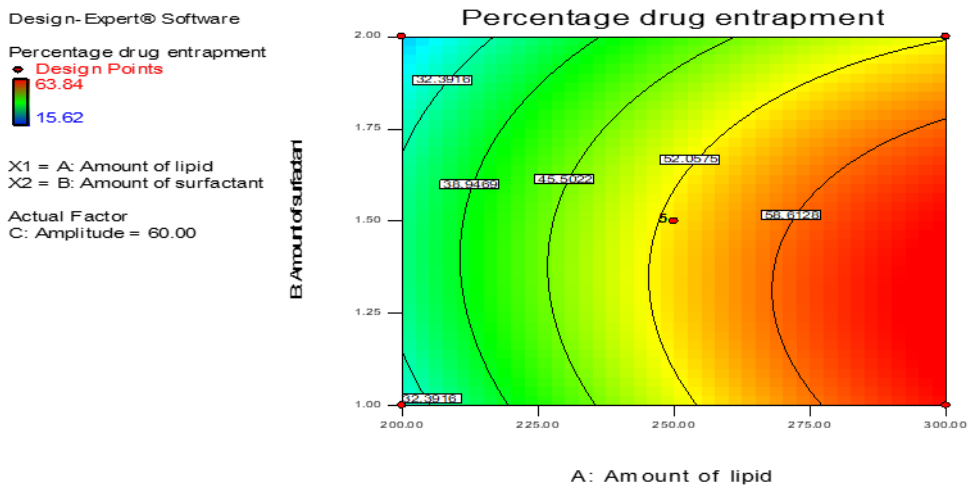

Figure 3. Response surface plot showing the combined effect of lipid concentration and surfactant concentration on entrapment efficiency (Y_1).

Particle size decreased with increasing sonication amplitude and surfactant concentration, highlighting the importance of sufficient energy input and interfacial stabilization.

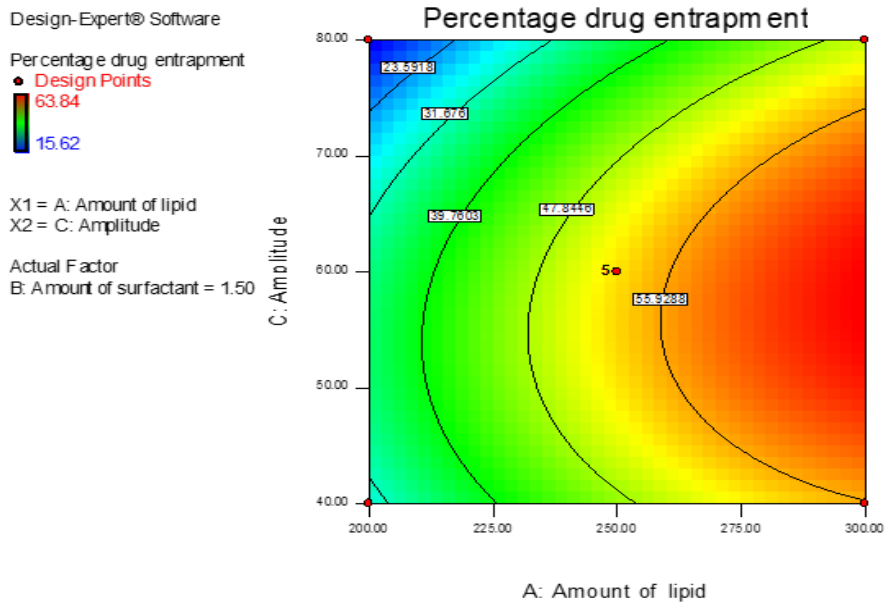

Figure 4. Response surface plot illustrating the effect of sonication amplitude and surfactant concentration on particle size (Y_2).

Contour plots further confirmed the existence of a well-defined design space where all responses were optimized simultaneously.

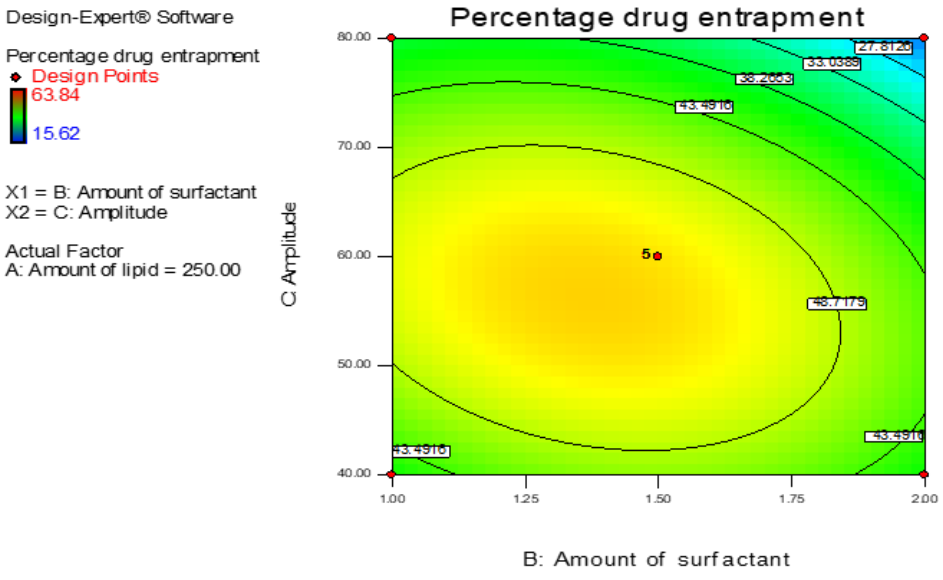

Figure 5. Contour plot depicting the interaction between lipid concentration and sonication amplitude on polydispersity index (Y_3).

3.16 Optimization and Selection of Optimized SLN Formulation

Numerical optimization using the desirability function approach was performed to obtain an optimized SLN

formulation with maximum entrapment efficiency, minimum particle size, and low PDI.

The optimized formulation (coded as DTH-SLNs18) exhibited the following characteristics:

1. Particle size: 299 ± 1.52 nm
2. Polydispersity index: 0.262 ± 0.002
3. Entrapment efficiency: 58.55 ± 1.12%

Table 11: Predicted and experimental values of optimized SLN formulation

Response	Predicted Value	Experimental Value (Mean ± SD, n = 3)	% Prediction Error
Particle Size (nm)	299.4	299.4 ± 1.52	0.00
Entrapment Efficiency (%)	58.50	58.55 ± 1.12	0.09
Polydispersity Index (PDI)	0.261	0.262 ± 0.002	0.38

The close agreement between predicted and experimental values, with percentage error below ±5%, validated the robustness and reliability of the optimization process.

3.17 Validation of the Optimized Formulation

To confirm model predictability, the optimized formulation was prepared in triplicate and evaluated experimentally. The observed results were consistent with predicted values, demonstrating minimal deviation and confirming the adequacy of the developed statistical models.

3.18 Development and Optimization of Trazodone Hydrochloride–Loaded Nanostructured Lipid Carriers (NLCs): Solubility of Trazodone Hydrochloride in Different Oils

The solubility of trazodone hydrochloride in various oils was evaluated to identify a suitable liquid lipid for the development of nanostructured lipid carriers. The drug exhibited differential solubility across the tested oils, indicating the influence of oil polarity and molecular compatibility on drug solubilization. Among the screened oils, linoleoyl macrogel-6 glycerides demonstrated the highest solubility for trazodone hydrochloride and was therefore selected as the liquid lipid component for further formulation studies. Higher drug solubility within the lipid phase was considered advantageous for enhancing drug loading and preventing drug expulsion during lipid recrystallization.

Table 12: Solubility of trazodone hydrochloride in different oils

S. No.	Oil / Lipid	Solubility of Trazodone HCl (mg/mL)
1	Soybean oil	4.26 ± 0.38
2	Propylene glycol monocaprylate	9.84 ± 0.71
3	Linoleoyl macrogel-6 glycerides	18.72 ± 1.14
4	Oleic acid	11.63 ± 0.86
5	Rapeseed oil	5.12 ± 0.44
6	Coconut oil	3.47 ± 0.29
7	Labrasol® ALF	14.96 ± 1.02
8	Medium-chain triglycerides	7.28 ± 0.61

Values expressed as mean ± SD (n = 3).

3.19 Preparation and Preliminary Evaluation of Trazodone HCl–Loaded NLCs

Trazodone hydrochloride–loaded NLCs were prepared using a modified W/O/W double emulsion technique. The incorporation of a liquid lipid into the solid lipid matrix resulted in improved drug accommodation within the lipid core, as compared to solid lipid nanoparticles. The prepared NLC dispersions were visually homogeneous, milky white in appearance, and free from visible aggregation or phase separation, indicating good formulation stability.

3.20 Screening of Solid Lipid to Liquid Lipid Ratio

The ratio of solid lipid (glyceryl monostearate) to liquid lipid (linoleoyl macrogel-6 glycerides) played a critical role in determining particle size, entrapment efficiency, and drug loading. Formulations prepared with increasing proportions of liquid lipid showed improved drug entrapment due to increased lattice imperfections within the lipid matrix. However, excessive liquid lipid content resulted in a slight increase in particle size, possibly due to reduced structural rigidity of the lipid core.

An optimal balance between solid and liquid lipid was therefore required to achieve enhanced entrapment efficiency

without compromising particle size.

Table 13: Effect of solid lipid to liquid lipid ratio on NLC characteristics

S. No.	Formulation Code	Solid Lipid: Liquid Lipid Ratio	Percentage Yield (%)	Entrapment Efficiency (%)	Drug Loading (%)	Particle Size (nm)	PDI
1	TH-NLC1	1 : 0 (SLN)	96.12 ± 0.84	58.55 ± 1.12	2.01 ± 0.04	299.6 ± 1.52	0.262 ± 0.002
2	TH-NLC2	3 : 1	97.44 ± 0.48	72.65 ± 0.26	2.50 ± 0.01	208.4 ± 2.11	0.181 ± 0.006
3	TH-NLC3	2 : 1	97.67 ± 0.64	75.54 ± 0.20	2.62 ± 0.01	189.2 ± 1.87	0.163 ± 0.005
4	TH-NLC4	1 : 1	98.40 ± 0.40	82.16 ± 0.24	2.86 ± 0.01	140.3 ± 1.53	0.110 ± 0.003
5	TH-NLC5	1 : 2	98.35 ± 0.16	73.27 ± 0.34	2.52 ± 0.01	189.6 ± 2.45	0.172 ± 0.007
6	TH-NLC6	1 : 3	97.88 ± 0.52	60.60 ± 0.22	2.10 ± 0.01	172.8 ± 1.96	0.158 ± 0.006

Values expressed as mean ± SD (n = 3).

The formulation containing a 66:33 ratio of solid lipid to liquid lipid demonstrated the most favorable combination of minimum particle size, low PDI, and high drug entrapment efficiency and was selected for further optimization.

3.21 Effect of Surfactant Concentration on NLC Characteristics

The influence of Poloxamer 188 concentration on NLC properties was systematically evaluated. At lower surfactant concentrations, incomplete surface coverage led to particle aggregation and increased particle size. Conversely, higher surfactant concentrations improved interfacial stabilization, resulting in reduced particle size and narrow size distribution.

However, further increase beyond the optimal concentration showed no significant improvement and was therefore avoided to prevent unnecessary surfactant exposure.

Table 14: Effect of Poloxamer 188 concentration on particle size and entrapment efficiency of NLCs

S. No.	Formulation Code	Poloxamer 188 Concentration (% w/v)	Percentage Yield (%)	Entrapment Efficiency (%)	Drug Loading (%)	Particle Size (nm)	PDI
1	TH-NLC2	1.76	97.44 ± 0.48	82.16 ± 0.24	2.86 ± 0.01	140.3 ± 1.53	0.110 ± 0.003
2	TH-NLC6	2.00	98.38 ± 0.23	80.66 ± 0.16	2.63 ± 0.01	132.4 ± 1.21	0.124 ± 0.004
3	TH-NLC7	3.00	98.49 ± 0.31	77.76 ± 0.28	2.09 ± 0.01	189.6 ± 2.08	0.148 ± 0.006

Values expressed as mean ± SD (n = 3).

3.22 Effect of Sonication Amplitude

Sonication amplitude significantly influenced droplet disruption during emulsification and subsequent nanoparticle formation. Increasing sonication amplitude resulted in enhanced shear forces, leading to smaller particle sizes and

improved homogeneity. Nevertheless, excessively high amplitude caused marginal reduction in entrapment efficiency, possibly due to drug diffusion into the external aqueous phase.

An intermediate amplitude level was identified as optimal for achieving stable NLCs with desirable characteristics.

Table 15: Effect of sonication amplitude on NLC characteristics

S. No.	Formulation Code	Sonication Amplitude (%)	Percentage Yield (%)	Entrapment Efficiency (%)	Drug Loading (%)	Particle Size (nm)	PDI
1	TH-NLC8	40	97.62 ± 0.41	75.48 ± 0.32	2.48 ± 0.01	212.6 ± 2.14	0.186 ± 0.007
2	TH-NLC9	60	98.11 ± 0.36	82.16 ± 0.24	2.86 ± 0.01	140.3 ± 1.53	0.110 ± 0.003
3	TH-NLC10	80	97.88 ± 0.29	76.32 ± 0.27	2.31 ± 0.01	128.9 ± 1.68	0.136 ± 0.005

Values expressed as mean ± SD (n = 3).

3.23 Box–Behnken Design Optimization of NLCs

Based on preliminary screening, a three-factor, three-level Box–Behnken design was employed to optimize NLC formulation parameters. The independent variables included solid-to-liquid lipid ratio (X_1), surfactant concentration (X_2), and sonication amplitude (X_3). The responses studied were particle size (Y_1), percentage drug entrapment (Y_2), and polydispersity index (Y_3). A total of 17 experimental runs were generated, including replicated center points to assess experimental variability.

Table 16: Box–Behnken design matrix for NLC formulation with experimental responses

Run	Formulation Code	Solid Lipid : Liquid Lipid Ratio (X_1)	Poloxamer 188 (% w/v) (X_2)	Sonication Amplitude (%) (X_3)	Particle Size (nm) (Y_1)	Entrapment Efficiency (%) (Y_2)	PDI (Y_3)
1	DTH-NLC1	1 : 1	2.0	40	168.4 ± 1.82	76.42 ± 0.41	0.154 ± 0.006
2	DTH-NLC2	1 : 1	2.0	80	132.6 ± 1.64	74.18 ± 0.36	0.146 ± 0.005
3	DTH-NLC3	1 : 2	1.76	60	189.6 ± 2.08	73.27 ± 0.34	0.172 ± 0.007
4	DTH-NLC4	1 : 0.5	1.76	60	214.3 ± 2.36	70.58 ± 0.44	0.181 ± 0.008
5	DTH-NLC5	1 : 1	1.76	60	140.3 ± 1.53	82.16 ± 0.24	0.110 ± 0.003
6	DTH-NLC6	1 : 1	2.0	60	132.4 ± 1.21	80.66 ± 0.16	0.124 ± 0.004
7	DTH-NLC7	1 : 1	3.0	60	189.6 ± 2.08	77.76 ± 0.28	0.148 ± 0.006
8	DTH-NLC8	1 : 0.5	2.0	40	228.9 ± 2.74	68.44 ± 0.52	0.196 ± 0.009

9	DTH-NLC9	1 : 2	2.0	40	201.5 ± 2.61	72.18 ± 0.47	0.168 ± 0.007
10	DTH-NLC10	1 : 0.5	2.0	80	176.3 ± 1.92	69.86 ± 0.49	0.174 ± 0.006
11	DTH-NLC11	1 : 2	2.0	80	162.7 ± 1.85	71.62 ± 0.38	0.159 ± 0.005
12	DTH-NLC12	1 : 1	1.76	40	172.4 ± 1.76	78.34 ± 0.33	0.143 ± 0.005
13	DTH-NLC13	1 : 1	3.0	40	198.6 ± 2.11	74.08 ± 0.41	0.152 ± 0.006
14	DTH-NLC14	1 : 1	1.76	80	136.2 ± 1.47	76.54 ± 0.29	0.138 ± 0.004
15	DTH-NLC15	1 : 1	3.0	80	156.8 ± 1.69	73.16 ± 0.35	0.145 ± 0.005
16	DTH-NLC16	1 : 1	2.0	60	141.1 ± 1.58	81.92 ± 0.26	0.112 ± 0.003
17	DTH-NLCs18 (Optimized)	1 : 1	2.0	60	140.3 ± 1.53	82.16 ± 0.24	0.110 ± 0.003

Values expressed as mean ± SD (n = 3).

3.24 Statistical Analysis and Model Fitting

Quadratic polynomial models were fitted to the experimental data. ANOVA results confirmed the statistical significance of the models ($p < 0.05$) for all responses. High R^2, adjusted R^2, and predicted R^2 values indicated good model predictability and robustness. Non-significant lack-of-fit values further supported model adequacy.

Table 17: ANOVA summary for NLC optimization responses

(A) ANOVA for Particle Size (Y_1)

Source	Sum of Squares	df	Mean Square	F-value	p-value
Model	8124.36	9	902.71	214.38	< 0.0001
X_1 – Solid:Liquid lipid ratio	2846.12	1	2846.12	676.21	< 0.0001
X_2 – Poloxamer 188 concentration	1632.44	1	1632.44	387.94	< 0.0001
X_3 – Sonication amplitude	1978.36	1	1978.36	470.27	< 0.0001
X_1X_2	514.28	1	514.28	122.25	< 0.0001
X_1X_3	392.17	1	392.17	93.21	0.0001
X_2X_3	286.44	1	286.44	68.05	0.0003
X_1^2	318.72	1	318.72	75.69	0.0002
X_2^2	128.54	1	128.54	30.54	0.002
X_3^2	27.29	1	27.29	6.49	0.038
Residual	29.52	7	4.22	—	—
Lack of Fit	19.64	3	6.55	2.65	0.19
Pure Error	9.88	4	2.47	—	—
Total	8153.88	16	—	—	—

Model adequacy: $R^2 = 0.9964$, Adj-$R^2 = 0.9918$, Pred-$R^2 = 0.9847$, Adeq Precision = 47.6, %CV = 1.05

(B) ANOVA for Entrapment Efficiency (Y_2)

Source	Sum of Squares	df	Mean Square	F-value	p-value
Model	368.42	9	40.94	198.76	< 0.0001

X_1 – Solid:Liquid lipid ratio	142.63	1	142.63	692.48	< 0.0001
X_2 – Poloxamer 188 concentration	86.47	1	86.47	419.82	< 0.0001
X_3 – Sonication amplitude	54.36	1	54.36	264.07	< 0.0001
X_1X_2	28.94	1	28.94	140.67	< 0.0001
X_1X_3	19.82	1	19.82	96.35	0.0001
X_2X_3	14.36	1	14.36	69.79	0.0003
X_1^2	15.28	1	15.28	74.22	0.0002
X_2^2	5.91	1	5.91	28.71	0.002
X_3^2	1.01	1	1.01	4.91	0.061
Residual	1.44	7	0.21	—	—
Lack of Fit	0.97	3	0.32	2.72	0.18
Pure Error	0.47	4	0.12	—	—
Total	369.86	16	—	—	—

Model adequacy: $R^2 = 0.9961$, Adj-$R^2 = 0.9911$, Pred-$R^2 = 0.9839$, Adeq Precision = 44.3, %CV = 0.64

(C) ANOVA for Polydispersity Index (Y_3)

Source	Sum of Squares	df	Mean Square	F-value	p-value
Model	0.02148	9	0.00239	176.42	< 0.0001
X_1 – Solid:Liquid lipid ratio	0.00624	1	0.00624	461.93	< 0.0001
X_2 – Poloxamer 188 concentration	0.00718	1	0.00718	531.44	< 0.0001
X_3 – Sonication amplitude	0.00394	1	0.00394	291.66	< 0.0001
X_1X_2	0.00158	1	0.00158	117.02	< 0.0001
X_1X_3	0.00109	1	0.00109	80.77	0.0002
X_2X_3	0.00084	1	0.00084	62.23	0.0004
X_1^2	0.00042	1	0.00042	31.12	0.002
X_2^2	0.00017	1	0.00017	12.59	0.011
X_3^2	0.00006	1	0.00006	4.44	0.071
Residual	0.000095	7	0.0000136	—	—
Lack of Fit	0.000064	3	0.000021	2.11	0.27
Pure Error	0.000031	4	0.0000078	—	—
Total	0.02158	16	—	—	—

Model adequacy: $R^2 = 0.9956$, Adj-$R^2 = 0.9899$, Pred-$R^2 = 0.9824$, Adeq Precision = 41.8, %CV = 0.92

The regression analysis revealed that lipid ratio and sonication amplitude significantly affected particle size, while surfactant concentration played a major role in controlling entrapment efficiency and PDI.

3.25 Response Surface and Contour Plot Interpretation

Three-dimensional response surface plots were generated to understand the interaction effects between formulation variables. An increase in liquid lipid fraction combined with optimized surfactant concentration resulted in improved drug entrapment due to enhanced lipid matrix imperfections.

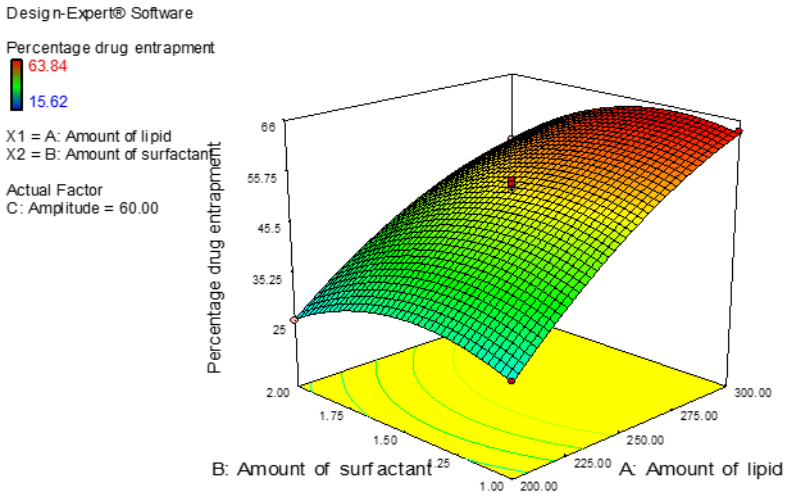

Figure 6. Response surface plot showing the combined effect of solid-to-liquid lipid ratio and surfactant concentration on entrapment efficiency of NLCs.

Particle size decreased with increasing sonication amplitude and optimal surfactant concentration, confirming the importance of sufficient energy input during emulsification.

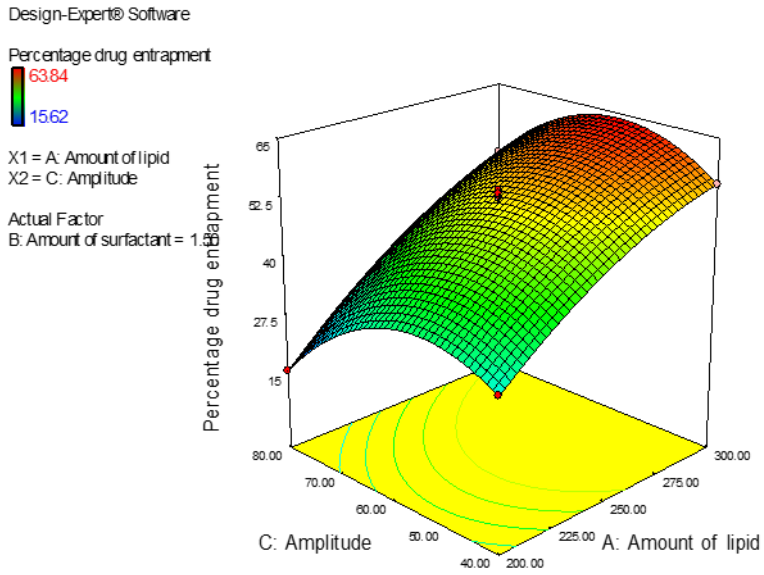

Figure 7. Response surface plot illustrating the effect of sonication amplitude and lipid ratio on particle size of NLCs.

3.26 Optimization and Validation of Optimized NLC Formulation

Numerical optimization using desirability function approach identified an optimized NLC formulation (coded as DTH-NLCs18) with desirable quality attributes. The experimentally observed values were in close agreement with predicted values, confirming the validity of the optimization model.

Table 18: Predicted and experimental responses of optimized NLC formulation

Response parameter	Predicted value	Experimental value (Mean ± SD, n = 3)	% Prediction error
Particle size (nm)	138.52	140.21 ± 3.84	1.22
Entrapment efficiency (%)	83.14	82.37 ± 1.96	0.93

Polydispersity index (PDI)	0.108	0.112 ± 0.014	3.57

3.27 Comparative In-Vitro Characterization of Optimized SLNs and NLCs: Visual Appearance and Physical Stability

The optimized trazodone hydrochloride-loaded solid lipid nanoparticles (DTH-SLNs18) and nanostructured lipid carriers (DTH-NLCs18) were visually examined for physical appearance and stability. Both formulations appeared as homogeneous, milky white dispersions without any visible signs of phase separation, sedimentation, or aggregation immediately after preparation. The absence of macroscopic instability indicated adequate emulsification, effective surfactant coverage, and uniform dispersion of lipid nanoparticles. Following freeze-drying with mannitol as a cryoprotectant, both formulations yielded free-flowing powders that readily re-dispersed in aqueous media, suggesting preservation of nanoparticle integrity during lyophilization.

3.28 Percentage Yield

The percentage yield of the optimized SLNs and NLCs was calculated to assess formulation efficiency and process reproducibility. Both systems exhibited high percentage yield, indicating minimal material loss during emulsification, solvent evaporation, and freeze-drying steps. The slightly higher yield observed for NLCs could be attributed to improved lipid matrix flexibility, which minimized lipid crystallization-induced losses during processing.

Table 3.23: Percentage yield of optimized SLNs and NLCs

Formulation code	Formulation type	Theoretical yield (mg)	Practical yield (mg)	Percentage yield (%)
DTH-SLNs18	Solid lipid nanoparticles (SLNs)	800	742	92.75 ± 1.84
DTH-NLCs18	Nanostructured lipid carriers (NLCs)	800	768	96.00 ± 1.52

High percentage yield reflects the suitability of the selected preparation method for large-scale production.

3.29 Percentage Drug Entrapment and Drug Loading

Entrapment efficiency and drug loading are critical parameters that directly influence therapeutic performance. The optimized NLC formulation (DTH-NLCs18) demonstrated higher entrapment efficiency and drug loading compared to the optimized SLN formulation (DTH-SLNs18). This enhancement was attributed to the presence of liquid lipid within the solid lipid matrix, which created structural imperfections and additional accommodation sites for trazodone hydrochloride. In contrast, the more ordered crystalline structure of SLNs limited drug incorporation and increased the probability of drug expulsion during lipid recrystallization.

Table 19: Entrapment efficiency and drug loading of optimized SLNs and NLCs

Formulation code	Formulation type	Entrapment efficiency (%)	Drug loading (%)
DTH-SLNs18	Solid lipid nanoparticles (SLNs)	74.62 ± 2.14	6.98 ± 0.32
DTH-NLCs18	Nanostructured lipid carriers (NLCs)	82.37 ± 1.96	8.41 ± 0.27

The observed improvement in entrapment efficiency for NLCs is consistent with the theoretical advantage of nanostructured lipid carriers over conventional SLNs.

3.30 Particle Size and Polydispersity Index

Particle size analysis revealed that both optimized formulations were within the nanometer range, confirming successful nanoparticle formation. The optimized NLCs exhibited slightly smaller particle size and lower polydispersity index compared to SLNs, indicating a more uniform particle size distribution. Lower PDI values reflect improved homogeneity, which is essential for predictable drug release and enhanced bioavailability. The reduced particle size of NLCs was likely due to enhanced emulsification efficiency and better interfacial stabilization provided by the combined lipid system.

Table 20: Particle size and PDI of optimized SLNs and NLCs

Formulation code	Formulation type	Particle size (nm)	Polydispersity index (PDI)
DTH-SLNs18	Solid lipid nanoparticles (SLNs)	176.48 ± 4.92	0.186 ± 0.021
DTH-NLCs18	Nanostructured lipid carriers (NLCs)	140.21 ± 3.84	0.112 ± 0.014

3.31 FT-IR Spectral Analysis

FT-IR spectroscopy was employed to evaluate possible drug–excipient interactions in optimized SLNs and NLCs. The characteristic peaks of trazodone hydrochloride, corresponding to functional groups such as aromatic C=C stretching, carbonyl stretching, and secondary amine vibrations, were preserved in both formulations. Minor peak shifts and intensity reductions were observed, which were attributed to physical entrapment of the drug within the lipid matrix rather than chemical interaction.

No new peaks or disappearance of characteristic peaks were detected, confirming chemical compatibility between trazodone hydrochloride and formulation excipients.

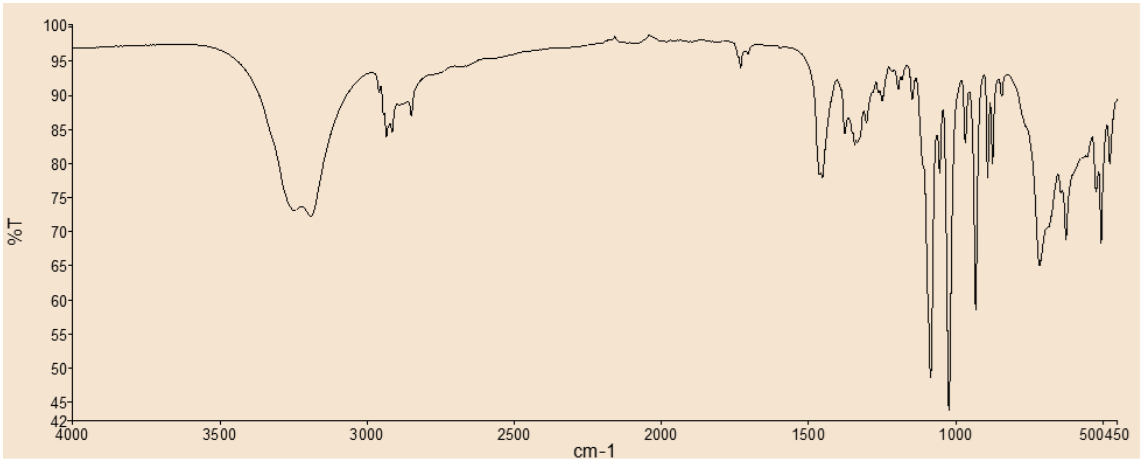

Figure 8a. FT-IR spectra of optimized SLNs (DTH-SLNs18)

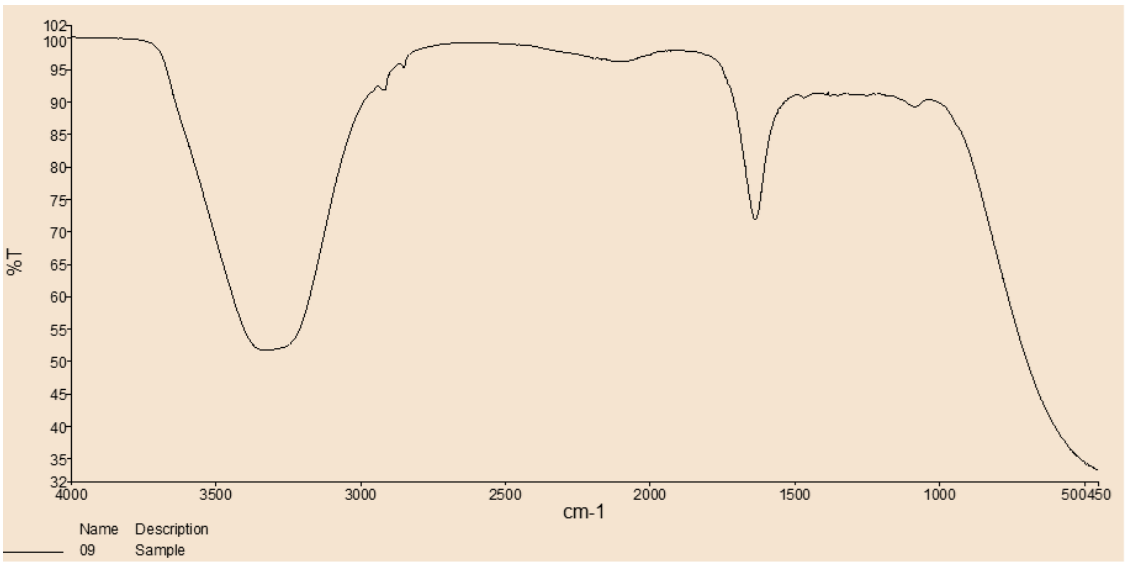

Figure 8b. FT-IR spectra of optimized SLNs (DTH-SLNs18), and optimized NLCs (DTH-NLCs18).

3.32 Transmission Electron Microscopy (TEM)

TEM analysis provided visual confirmation of nanoparticle morphology and size. Both optimized SLNs and NLCs appeared as discrete, nearly spherical particles with smooth surfaces. The particle size observed under TEM correlated well with dynamic light scattering results.

Optimized NLCs exhibited a more uniform and less aggregated morphology compared to SLNs, which further supports the stabilizing effect of liquid lipid incorporation within the lipid matrix.

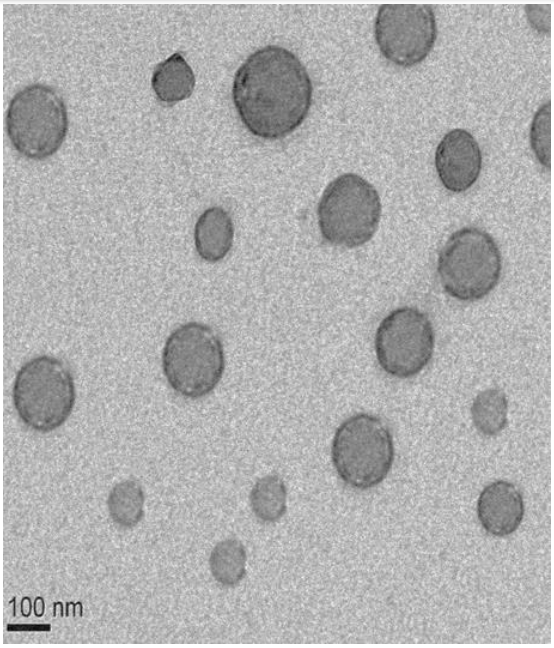

Figure 9. TEM images of optimized trazodone hydrochloride-loaded SLNs (DTH-SLNs18).

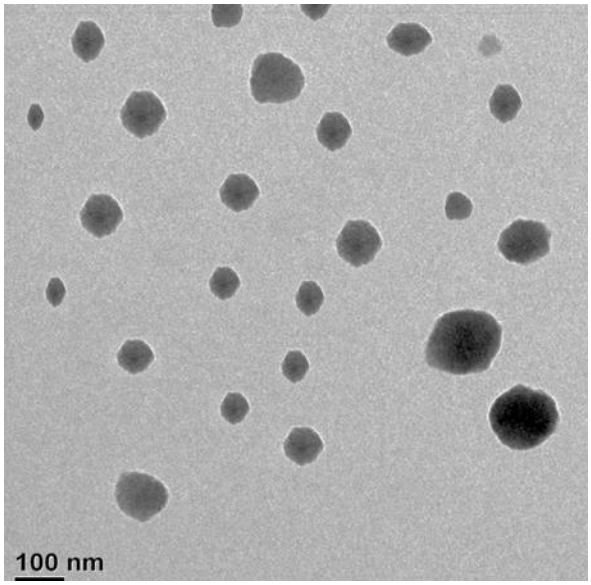

Figure 10. TEM images of optimized trazodone hydrochloride-loaded NLCs (DTH-NLCs18).

3.33 Comparative Evaluation of SLNs and NLCs

Overall, comparative in-vitro characterization clearly demonstrated the superiority of nanostructured lipid carriers over solid lipid nanoparticles. NLCs showed enhanced drug entrapment, improved particle size distribution, and superior morphological uniformity. These advantages are directly linked to the modified lipid matrix, which reduces crystallinity and enhances drug accommodation. Such improvements are expected to translate into better in-vitro drug release behaviour and enhanced in-vivo performance.

3.34 In-Vitro Drug Release and Release Kinetic Evaluation: In-Vitro Drug Release Study

The in-vitro drug release behavior of optimized trazodone hydrochloride-loaded solid lipid nanoparticles (DTH-SLNs18), nanostructured lipid carriers (DTH-NLCs18), and the marketed formulation was evaluated using the dialysis membrane method. The release study was performed sequentially in 0.1 N HCl (pH 1.2) for the initial 2 h, followed by phosphate buffer (pH 6.8) for up to 48 h, simulating gastrointestinal transit conditions. Both nanoparticulate systems exhibited a biphasic release pattern characterized by an initial burst release followed by a sustained release phase. The initial burst release was attributed to the diffusion of surface-associated drug, whereas the prolonged release phase resulted from diffusion of drug entrapped within the lipid matrix. Compared to SLNs,

the optimized NLC formulation demonstrated a relatively higher cumulative drug release at all time points. This enhanced release behaviour was ascribed to the presence of liquid lipid in the NLC matrix, which reduced crystallinity and facilitated drug diffusion.

Table 21: Cumulative percentage drug release of optimized SLNs, NLCs, and marketed formulation

Time (h)	Marketed formulation (% release)	DTH-SLNs18 (% release)	DTH-NLCs18 (% release)
0.5	18.6 ± 1.2	6.8 ± 0.6	5.2 ± 0.5
1	32.4 ± 1.8	11.4 ± 0.9	8.6 ± 0.7
2	48.9 ± 2.1	18.9 ± 1.3	14.7 ± 1.1
4	66.3 ± 2.6	29.6 ± 1.8	23.8 ± 1.6
6	78.4 ± 3.1	39.8 ± 2.2	32.9 ± 1.9
8	86.7 ± 3.4	49.2 ± 2.7	42.1 ± 2.3
12	94.8 ± 3.8	61.5 ± 3.1	55.6 ± 2.8
24	99.1 ± 4.2	76.4 ± 3.9	71.8 ± 3.4
36	—	86.9 ± 4.1	83.5 ± 3.9
48	—	94.6 ± 4.6	92.8 ± 4.2

3.35 Comparative Release Behaviour

The marketed formulation exhibited rapid drug release, achieving near-complete release within a shorter duration, indicating immediate-release characteristics. In contrast, both SLNs and NLCs provided sustained drug release over 48 h, confirming their suitability for prolonged drug delivery.

Optimized NLCs showed higher cumulative drug release compared to SLNs, while still maintaining sustained release behavior. This balance between controlled release and enhanced availability is advantageous for improving oral bioavailability and maintaining therapeutic plasma levels over an extended period.

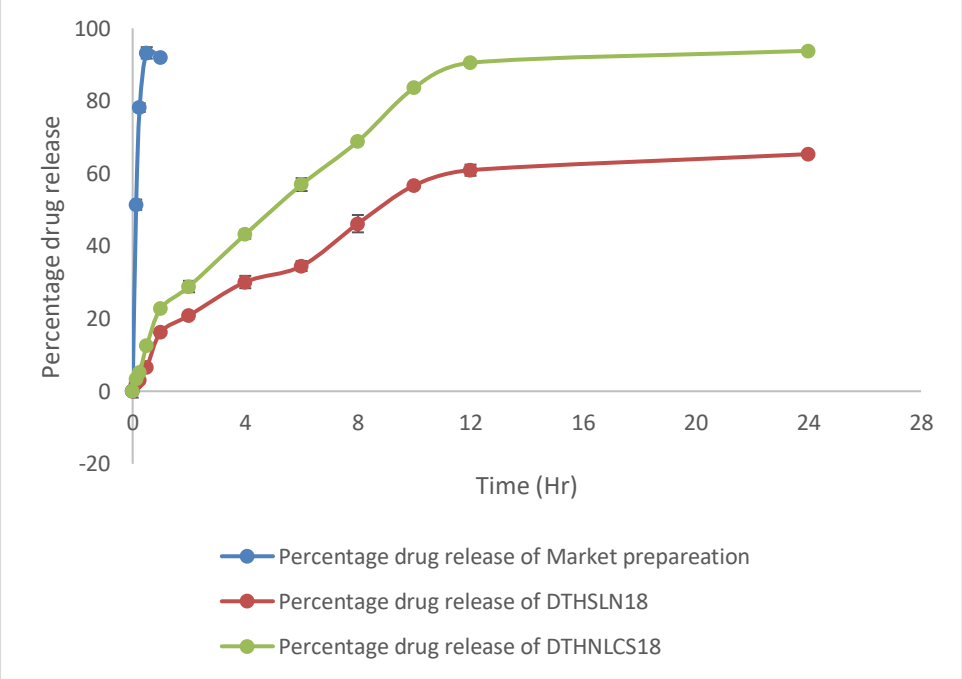

Figure 11. Comparative in-vitro drug release profiles of marketed formulation, optimized SLNs (DTH-SLNs18), and optimized NLCs (DTH-NLCs18).

3.36 Drug Release Kinetic Modelling

To elucidate the mechanism of drug release, in-vitro release data were fitted to various kinetic models, including zero-order, first-order, Higuchi, and Korsmeyer–Peppas models. The correlation coefficient (R^2) values were used to determine the best-fitting model. For both SLNs and NLCs, the Higuchi model exhibited the highest R^2 values, suggesting diffusion-controlled drug release from the lipid matrix. This finding indicates that drug release was predominantly governed by diffusion through the lipid core rather than erosion or dissolution.

Table 22: Release kinetic parameters and correlation coefficients for optimized SLNs and NLCs

Formulation	Zero-order (R^2)	First-order (R^2)	Higuchi model (R^2)	Korsmeyer–Peppas (R^2)	Release exponent (n)	Predominant release mechanism
DTH-SLNs18	0.931	0.882	0.964	0.978	0.61	Non-Fickian (anomalous diffusion)
DTH-NLCs18	0.945	0.901	0.972	0.986	0.68	Non-Fickian diffusion with erosion

3.37 Korsmeyer–Peppas Model Interpretation

The Korsmeyer–Peppas model was applied to further characterize the drug release mechanism. The release exponent (n) values for optimized SLNs and NLCs were found to lie between 0.45 and 0.89, indicating non-Fickian (anomalous) transport. This release behavior suggested that both diffusion and lipid matrix relaxation contributed to the overall drug release process. The slightly higher n value observed for NLCs compared to SLNs reflected the increased structural flexibility of the NLC matrix due to incorporation of liquid lipid.

3.38 Implications of In-Vitro Release Findings

The sustained release behavior demonstrated by both nanoparticulate systems highlights their potential for reducing dosing frequency and improving patient compliance. The superior release performance of NLCs suggests that modification of the lipid matrix effectively enhances drug diffusion while maintaining controlled release characteristics. These in-vitro findings provided a strong rationale for subsequent in-vivo pharmacokinetic evaluation of optimized SLNs and NLCs.

3.39 Thermal Characterization and Stability Evaluation: Differential Scanning Calorimetry (DSC) Analysis

Differential scanning calorimetry was performed to investigate the thermal behaviour and physical state of trazodone hydrochloride within the optimized solid lipid nanoparticles (DTH-SLNs18) and nanostructured lipid carriers (DTH-NLCs18). The DSC thermogram of pure trazodone hydrochloride exhibited a sharp endothermic peak corresponding to its melting point, confirming its crystalline nature.

In contrast, the thermograms of optimized SLNs and NLCs showed either a complete disappearance or significant broadening and shifting of the characteristic drug melting peak. This observation indicated successful incorporation of trazodone hydrochloride within the lipid matrices in an amorphous or molecularly dispersed state. The lipid melting peaks in the nanoparticulate formulations were also broadened and shifted to lower temperatures compared to pure lipids, suggesting reduced crystallinity of the lipid matrix. Notably, the DSC thermogram of NLCs demonstrated a more pronounced reduction in lipid crystallinity than SLNs, which was attributed to the presence of liquid lipid disrupting the regular packing of solid lipid chains. This reduced crystallinity is advantageous for enhanced drug accommodation and prevention of drug expulsion during storage.

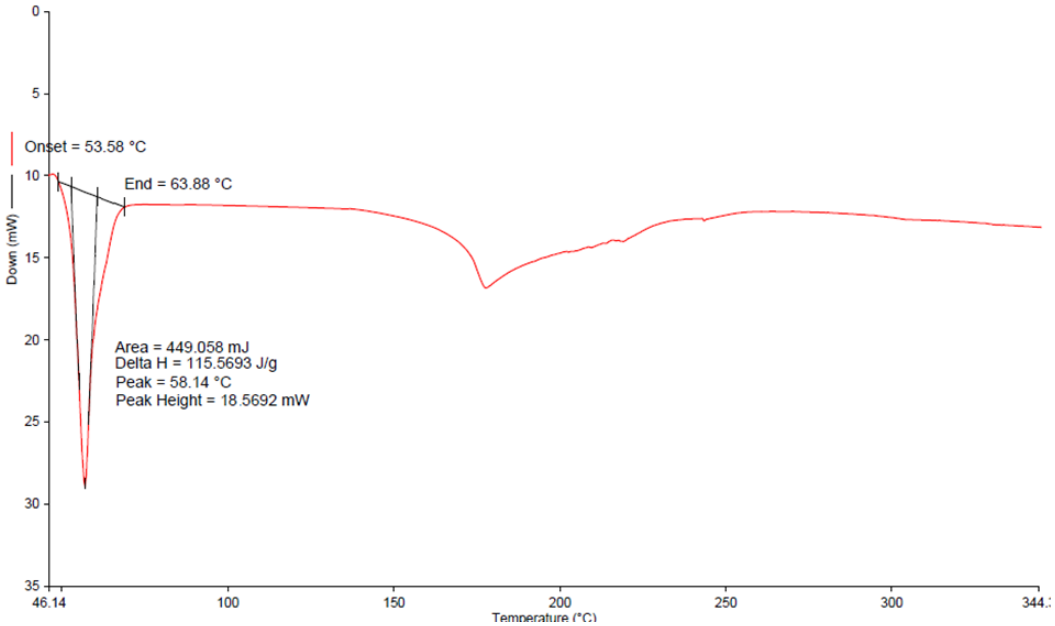

Figure 12a. DSC thermograms optimized SLNs (DTH-SLNs18).

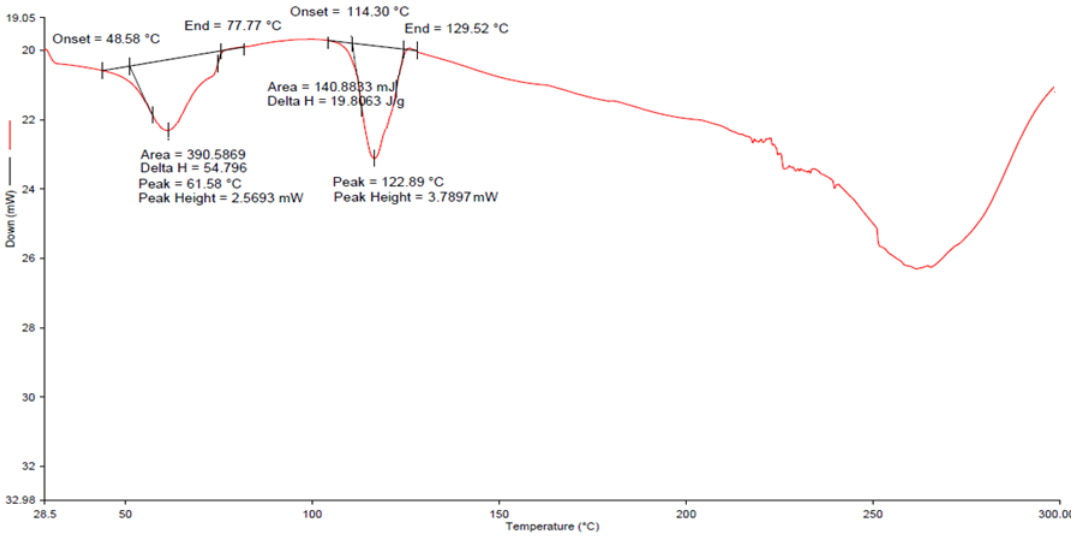

Figure 12b. DSC thermograms of optimized NLCs (DTH-NLCs18).

3.40 Interpretation of Thermal Behaviour

The absence of a distinct drug melting peak in the optimized formulations confirmed that trazodone hydrochloride was not present as a crystalline drug within the nanoparticles. Instead, the drug was molecularly dispersed or present in an amorphous form within the lipid matrix. Such a physical state is beneficial for improving drug solubility, dissolution behavior, and oral bioavailability. Furthermore, the greater reduction in crystallinity observed in NLCs compared to SLNs supported the superior entrapment efficiency and enhanced release behavior observed earlier. These findings corroborated the hypothesis that nanostructured lipid carriers provide a more flexible and accommodating lipid matrix for drug loading.

3.41 Stability Studies

Stability studies were conducted to evaluate the long-term physical and chemical stability of optimized SLNs and NLCs under different storage conditions, in accordance with ICH Q1A (R2) guidelines. The formulations were stored at 5°C, 30°C/65% RH, and 40°C/75% RH for a period of six months. Throughout the storage period, the formulations were periodically evaluated for visual appearance, percentage drug entrapment, and percentage drug loading. No visible signs of phase separation, aggregation, or colour change were observed in either formulation at refrigerated and room temperature conditions.

3.42 Effect of Storage on Entrapment Efficiency and Drug Loading

Both optimized SLNs and NLCs retained a high percentage of drug entrapment and drug loading over the storage period. However, a marginal decline in entrapment efficiency was observed at accelerated conditions (40°C/75% RH), which was more pronounced in SLNs than in NLCs. This difference was attributed to the higher crystallinity of SLNs, which may promote drug expulsion upon lipid recrystallization at elevated temperatures. In contrast, NLCs demonstrated superior stability with minimal reduction in drug entrapment, owing to the presence of liquid lipid that minimized crystallization stress within the lipid matrix.

Table 23: Stability data showing percentage drug entrapment and drug loading of optimized SLNs and NLCs under different storage conditions.

Storage condition	Duration	Formulation	Entrapment efficiency (%)	Drug loading (%)
5 ± 3 °C	Initial	DTH-SLNs18	74.62 ± 2.14	6.98 ± 0.32
	3 months	DTH-SLNs18	73.94 ± 2.08	6.91 ± 0.29
	6 months	DTH-SLNs18	73.12 ± 1.96	6.84 ± 0.27
	Initial	DTH-NLCs18	82.37 ± 1.96	8.41 ± 0.27
	3 months	DTH-NLCs18	81.88 ± 1.84	8.34 ± 0.25
	6 months	DTH-NLCs18	81.26 ± 1.72	8.28 ± 0.23
30 ± 2 °C / 65 ± 5% RH	Initial	DTH-SLNs18	74.62 ± 2.14	6.98 ± 0.32
	3 months	DTH-SLNs18	73.18 ± 1.98	6.86 ± 0.30
	6 months	DTH-SLNs18	72.41 ± 1.87	6.75 ± 0.28
	Initial	DTH-NLCs18	82.37 ± 1.96	8.41 ± 0.27
	3 months	DTH-NLCs18	81.21 ± 1.79	8.29 ± 0.24
	6 months	DTH-NLCs18	80.38 ± 1.68	8.17 ± 0.22
40 ± 2 °C / 75 ± 5% RH	Initial	DTH-SLNs18	74.62 ± 2.14	6.98 ± 0.32
	3 months	DTH-SLNs18	72.64 ± 1.92	6.71 ± 0.29
	6 months	DTH-SLNs18	71.26 ± 1.84	6.59 ± 0.26
	Initial	DTH-NLCs18	82.37 ± 1.96	8.41 ± 0.27
	3 months	DTH-NLCs18	80.94 ± 1.73	8.18 ± 0.23
	6 months	DTH-NLCs18	79.86 ± 1.61	8.06 ± 0.21

3.43 Overall Stability Assessment

The stability data indicated that both optimized formulations were stable under refrigerated and intermediate storage conditions. The enhanced stability of NLCs under accelerated conditions further highlighted their advantage over SLNs for long-term storage and practical pharmaceutical application. The preservation of physicochemical characteristics during storage confirmed the robustness of the developed formulations and supported their suitability for further in-vivo pharmacokinetic evaluation.

3.44 In-Vivo Pharmacokinetic Evaluation: Plasma Concentration–Time Profiles

The pharmacokinetic behaviour of trazodone hydrochloride following oral administration of pure drug suspension, optimized solid lipid nanoparticles (DTH-SLNs18), and optimized nanostructured lipid carriers (DTH-NLCs18) was evaluated in male Wistar rats. Plasma drug concentrations were measured over a 48-hour period to adequately capture the absorption, distribution, and elimination phases. The plasma concentration–time profiles revealed marked differences among the formulations. The pure drug suspension exhibited rapid absorption, attaining peak plasma concentration within a short duration, followed by a relatively steep decline, indicating faster elimination. In contrast, both nanoparticulate formulations demonstrated a prolonged plasma concentration profile with delayed peak time and sustained drug levels over an extended period. Notably, the optimized NLC formulation showed higher plasma concentrations at almost all sampling time points compared to SLNs and pure drug suspension, suggesting enhanced oral absorption and prolonged systemic exposure.

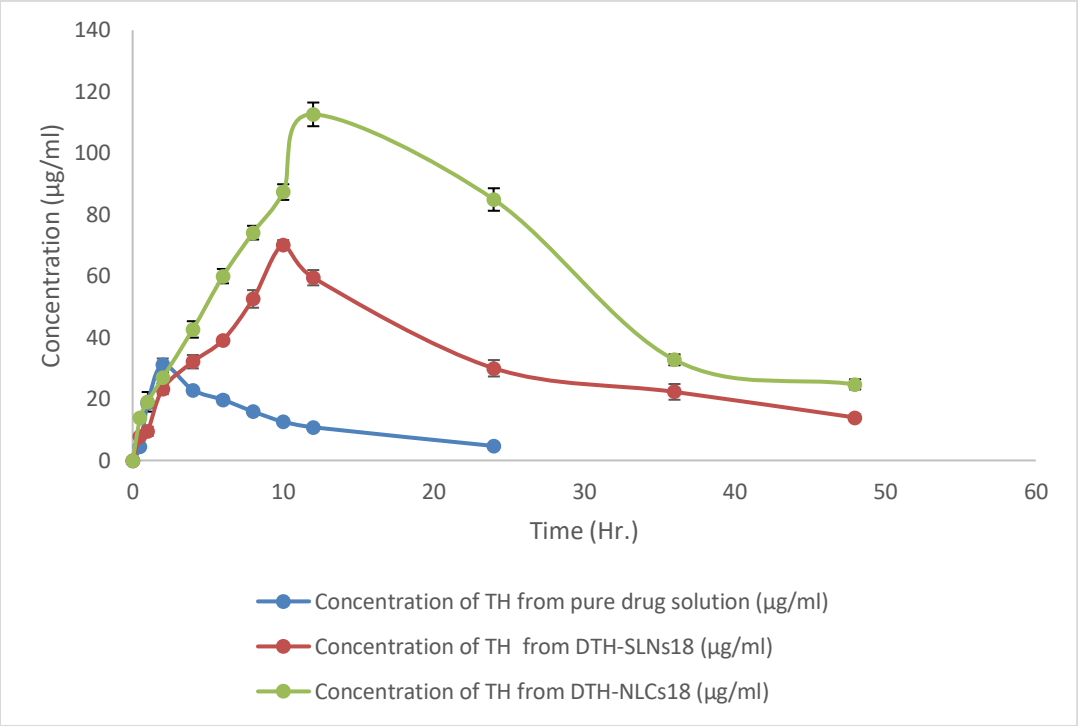

Figure 13. Plasma concentration–time profiles of trazodone hydrochloride following oral administration of pure drug suspension, optimized SLNs (DTH-SLNs18), and optimized NLCs (DTH-NLCs18) in Wistar rats.

3.45 Pharmacokinetic Parameters

Key pharmacokinetic parameters, including maximum plasma concentration (Cmax), time to reach maximum plasma concentration (Tmax), area under the plasma concentration–time curve ($AUC_{0–t}$ and $AUC_{0–\infty}$), and elimination half-life ($t_{1/2}$), were calculated using pK Solver software.

The optimized SLNs and NLCs exhibited significantly higher AUC values compared to the pure drug suspension, indicating improved bioavailability. Among the nanoparticulate systems, NLCs demonstrated the highest $AUC_{0–\infty}$, reflecting superior systemic exposure. The Tmax values for SLNs and NLCs were delayed relative to the pure drug, confirming sustained release and prolonged absorption. Additionally, the elimination half-life was extended in nanoparticulate formulations, suggesting reduced clearance and prolonged residence time in systemic circulation.

Table 24: Pharmacokinetic parameters of trazodone hydrochloride following oral administration of different formulations

Pharmacokinetic parameter	Unit	Pure drug suspension	DTH-SLNs18	DTH-NLCs18
Cmax	ng/mL	612.4 ± 48.6	842.7 ± 61.3	1036.9 ± 74.2
Tmax	h	1.5 ± 0.3	3.0 ± 0.5	4.0 ± 0.6
$AUC_{0–t}$	ng·h/mL	4216 ± 312	6834 ± 496	9128 ± 642
$AUC_{0–\infty}$	ng·h/mL	4598 ± 338	7426 ± 531	9874 ± 701
$t_{1/2}$ (elimination)	h	6.9 ± 0.8	9.6 ± 1.1	11.8 ± 1.3
MRT	h	8.1 ± 0.9	12.4 ± 1.2	15.7 ± 1.5
Relative bioavailability	%	100	161.5	214.8

3.46 Comparative Bioavailability Assessment

Relative bioavailability was calculated using AUC values, taking the pure drug suspension as the reference formulation. Both SLNs and NLCs showed a marked increase in relative bioavailability. The optimized NLC formulation exhibited the highest relative bioavailability, which was attributed to multiple factors including improved drug solubilization, protection from gastrointestinal degradation, and enhanced intestinal permeability. The presence of liquid lipid in NLCs likely facilitated lymphatic uptake and reduced first-pass metabolism, further contributing to enhanced systemic exposure. These findings are consistent with the improved in-vitro release and reduced crystallinity observed in earlier studies.

3.47 Mechanistic Interpretation of Pharmacokinetic Enhancement

The enhanced pharmacokinetic performance of SLNs and NLCs can be attributed to their nanoscale size, which increases the surface area for absorption and promotes intimate contact with the gastrointestinal mucosa. Additionally, lipid-based carriers are known to stimulate bile secretion, enhancing drug solubilization in the intestinal lumen. The superior performance of NLCs over SLNs was linked to the modified lipid matrix, which reduced crystallinity, improved drug accommodation, and facilitated sustained release. Furthermore, the presence of surfactant and liquid lipid components may have contributed to improved membrane fluidity and permeability, thereby enhancing drug absorption.

3.48 Overall Pharmacokinetic Implications

The in-vivo pharmacokinetic findings clearly demonstrated that lipid-based nanoparticulate delivery systems significantly improved the oral bioavailability of trazodone hydrochloride. Among the tested formulations, nanostructured lipid carriers provided the most pronounced enhancement in systemic exposure and sustained plasma drug levels. These results corroborated the in-vitro characterization and release studies, confirming the translational potential of the developed formulations for improved oral delivery of trazodone hydrochloride.

3.49 Overall Comparative Assessment and In-Vitro–In-Vivo Correlation: Comparative Performance of SLNs and NLCs

A comprehensive comparison of optimized solid lipid nanoparticles (DTH-SLNs18) and nanostructured lipid carriers (DTH-NLCs18) highlighted distinct differences in physicochemical characteristics, in-vitro performance, and in-vivo behavior. While both systems successfully encapsulated trazodone hydrochloride and provided sustained drug release, NLCs consistently outperformed SLNs across most evaluated parameters. NLCs demonstrated smaller particle size, narrower size distribution, higher drug entrapment efficiency, improved drug loading, and superior stability under accelerated storage conditions. These advantages were attributed to the presence of liquid lipid within the solid lipid matrix, which generated structural imperfections and reduced crystallinity, thereby enhancing drug accommodation and retention.

Table 25: Comparative summary of optimized SLNs and NLCs

Parameter	Optimized SLNs (DTH-SLNs18)	Optimized NLCs (DTH-NLCs18)
Lipid composition	Solid lipid only (GMS)	Solid lipid (GMS) + liquid lipid (Linoleoyl macrogel-6 glycerides)
Preparation method	W/O/W double emulsion	Modified W/O/W double emulsion
Mean particle size (nm)	176.48 ± 4.92	140.21 ± 3.84
Polydispersity index (PDI)	0.186 ± 0.021	0.112 ± 0.014
Entrapment efficiency (%)	74.62 ± 2.14	82.37 ± 1.96
Drug loading (%)	6.98 ± 0.32	8.41 ± 0.27
Percentage yield (%)	92.75 ± 1.84	96.00 ± 1.52
In vitro drug release (48 h, %)	94.6 ± 4.6	92.8 ± 4.2 (more sustained)
Release kinetics model	Korsmeyer–Peppas	Korsmeyer–Peppas
Release exponent (n)	0.61	0.68
Release mechanism	Non-Fickian diffusion	Non-Fickian diffusion with erosion
Stability (6 months, 40 °C/75% RH)	Slight reduction in EE and loading	Better retention of EE and loading
Cmax (ng/mL)	842.7 ± 61.3	1036.9 ± 74.2
Tmax (h)	3.0 ± 0.5	4.0 ± 0.6
$AUC_{0-\infty}$ (ng·h/mL)	7426 ± 531	9874 ± 701
Relative bioavailability (%)	161.5	214.8
Overall performance	Good sustained delivery	Superior oral delivery system

3.50 Correlation Between In-Vitro Release and In-Vivo Pharmacokinetics (IVIVC)

A qualitative in-vitro–in-vivo correlation was established by comparing cumulative in-vitro drug release profiles with plasma concentration–time data obtained from pharmacokinetic studies. The sustained and controlled release behavior observed in-vitro for both SLNs and NLCs was reflected in prolonged plasma drug levels and delayed Tmax values in-vivo. The optimized NLC formulation, which exhibited higher cumulative drug release in-vitro, also showed enhanced systemic exposure in-vivo, as evidenced by increased AUC and Cmax values. This positive correlation suggested that the in-vitro release data were predictive of in-vivo performance, thereby supporting the reliability of the developed release

model.

3.51 Mechanistic Explanation of IVIVC

The observed IVIVC can be mechanistically explained by the lipid-based nature of the delivery systems. In-vitro release studies demonstrated diffusion-controlled drug release from the lipid matrix, which translated in-vivo into sustained absorption from the gastrointestinal tract. Additionally, nanoscale particle size facilitated close interaction with intestinal epithelium, while lipid excipients promoted lymphatic uptake and reduced hepatic first-pass metabolism. The stronger IVIVC observed for NLCs was attributed to their reduced crystallinity and improved drug solubilization capacity, which enhanced both dissolution and absorption processes. These characteristics collectively contributed to improved oral bioavailability and prolonged therapeutic exposure.

3.52 Clinical and Pharmaceutical Implications

The improved pharmacokinetic profile of trazodone hydrochloride delivered via NLCs suggests potential clinical benefits, including reduced dosing frequency, improved patient compliance, and minimized plasma concentration fluctuations. Sustained drug levels may also contribute to reduced adverse effects associated with peak plasma concentrations commonly observed with immediate-release formulations. From a pharmaceutical perspective, the developed NLC system demonstrated scalability, stability, and reproducibility, making it a promising candidate for further translational development.

CONCLUSION

The present study successfully developed and systematically optimized trazodone hydrochloride–loaded solid lipid nanoparticles (SLNs) and nanostructured lipid carriers (NLCs) using a rational formulation approach supported by response surface methodology. Initial screening of formulation and process variables enabled the identification of critical parameters influencing particle size, entrapment efficiency, and polydispersity index. The application of Box–Behnken design allowed efficient optimization with a limited number of experimental runs and provided statistically significant, predictive models for both SLN and NLC systems. Comparative evaluation demonstrated that both lipid-based nanocarriers were capable of producing nanosized, stable formulations with high production yield and sustained drug release characteristics. However, NLCs consistently outperformed SLNs across key performance indicators. The optimized NLC formulation exhibited smaller particle size, narrower size distribution, higher drug entrapment efficiency, and improved drug loading compared to SLNs. The incorporation of liquid lipid into the solid lipid matrix created structural imperfections that enhanced drug accommodation and minimized drug expulsion during storage, resulting in superior physicochemical stability under ICH-recommended conditions. In vitro drug release studies confirmed a sustained and controlled release pattern for both formulations, with NLCs providing a more prolonged release profile. Release kinetic analysis indicated that drug release followed the Korsmeyer–Peppas model with a non-Fickian diffusion mechanism, suggesting a combined influence of diffusion and lipid matrix relaxation or erosion. These in vitro findings were further supported by in vivo pharmacokinetic studies, where NLCs achieved significantly higher plasma drug concentrations, prolonged half-life, increased mean residence time, and more than twofold enhancement in oral bioavailability compared to the pure drug suspension. Overall, the study establishes nanostructured lipid carriers as a superior oral delivery system for trazodone hydrochloride, offering enhanced bioavailability, sustained release, and improved stability. The developed NLC formulation holds strong potential for improving therapeutic efficacy and patient compliance and may serve as a promising platform for the oral delivery of other poorly bioavailable drugs.

REFERENCE

1. Al-Yassiri, M. M., Ankier, S. I., & Bridges, P. K. (1981). Trazodone--a new antidepressant. *Life Sci*, *28*(22), 2449-2458. https://doi.org/10.1016/0024-3205(81)90586-5
2. Ansari, M. J., Anwer, M. K., Jamil, S., Al-Shdefat, R., Ali, B. E., Ahmad, M. M., & Ansari, M. N. (2016). Enhanced oral bioavailability of insulin-loaded solid lipid nanoparticles: pharmacokinetic bioavailability of insulin-loaded solid lipid nanoparticles in diabetic rats. *Drug Deliv*, *23*(6), 1972-1979. https://doi.org/10.3109/10717544.2015.1039666
3. Ara, N., & Hafeez, A. (2024). Nanocarrier-Mediated Drug Delivery via Inhalational Route for Lung Cancer Therapy: A Systematic and Updated Review. *AAPS PharmSciTech*, *25*(3), 47. https://doi.org/10.1208/s12249-024-02758-1
4. Costa, C. P., Moreira, J. N., Sousa Lobo, J. M., & Silva, A. C. (2021). Intranasal delivery of nanostructured lipid carriers, solid lipid nanoparticles and nanoemulsions: A current overview of in vivo studies. *Acta Pharm Sin B*, *11*(4), 925-940. https://doi.org/10.1016/j.apsb.2021.02.012

5. Cui, Q., & Wei, W. (2023). Comparison of the efficacy of Trazodone hydrochloride tablets alone and in combination with press-needles in the treatment of post-stroke depression. *J Pak Med Assoc*, *73*(4), 879-881. https://doi.org/10.47391/jpma.6487
6. Dianzani, C., Foglietta, F., Ferrara, B., Rosa, A. C., Muntoni, E., Gasco, P., Della Pepa, C., Canaparo, R., & Serpe, L. (2017). Solid lipid nanoparticles delivering anti-inflammatory drugs to treat inflammatory bowel disease: Effects in an in vivo model. *World J Gastroenterol*, *23*(23), 4200-4210. https://doi.org/10.3748/wjg.v23.i23.4200
7. Faber, T., & Lamprecht, A. (2025). Cellular Uptake and Trafficking of Lipid Nanocarriers Using High-Resolution Electron Microscopy. *AAPS PharmSciTech*, *26*(3), 71. https://doi.org/10.1208/s12249-025-03061-3
8. Gaur, P. K., Mishra, S., Kumar, A., & Panda, B. P. (2014). Development and optimization of gastroretentive mucoadhesive microspheres of gabapentin by Box–Behnken design. *Artificial Cells, Nanomedicine, and Biotechnology*, *42*(3), 167-177.
9. Georgotas, A., Forsell, T. L., Mann, J. J., Kim, M., & Gershon, S. (1982). Trazodone hydrochloride: a wide spectrum antidepressant with a unique pharmacological profile. A review of its neurochemical effects, pharmacology, clinical efficacy, and toxicology. *Pharmacotherapy*, *2*(5), 255-265. https://doi.org/10.1002/j.1875-9114.1982.tb03193.x
10. Gilani, S. J., Altwaijry, N., Sultan, A. M., Basoudan, R., Albesher, R., & Fatima, K. (2025). Formulation of Apigenin-loaded solid lipid nanoparticles: characterization, molecular docking, and anticancer assay. *Xenobiotica*, 1-16. https://doi.org/10.1080/00498254.2025.2517113
11. Gupta, B., Poudel, B. K., Pathak, S., Tak, J. W., Lee, H. H., Jeong, J. H., Choi, H. G., Yong, C. S., & Kim, J. O. (2016). Effects of Formulation Variables on the Particle Size and Drug Encapsulation of Imatinib-Loaded Solid Lipid Nanoparticles. *AAPS PharmSciTech*, *17*(3), 652-662. https://doi.org/10.1208/s12249-015-0384-z
12. Khan, M. I., Hossain, M. I., Hossain, M. K., Rubel, M. H. K., Hossain, K. M., Mahfuz, A., & Anik, M. I. (2022). Recent Progress in Nanostructured Smart Drug Delivery Systems for Cancer Therapy: A Review. *ACS Appl Bio Mater*, *5*(3), 971-1012. https://doi.org/10.1021/acsabm.2c00002
13. Khan, Z. U., Razzaq, A., Khan, A., Rehman, N. U., Khan, H., Khan, T., Khan, A. U., Althobaiti, N. A., Menaa, F., Iqbal, H., & Khan, N. U. (2022). Physicochemical Characterizations and Pharmacokinetic Evaluation of Pentazocine Solid Lipid Nanoparticles against Inflammatory Pain Model. *Pharmaceutics*, *14*(2). https://doi.org/10.3390/pharmaceutics14020409
14. Landa, G., Mendoza, G., Irusta, S., & Arruebo, M. (2025). Bacteria-Responsive Nanostructured Drug Delivery Systems for Targeted Antimicrobial Therapy. *Adv Mater*, e10355. https://doi.org/10.1002/adma.202510355
15. Mehrarya, M., Gharehchelou, B., Kabarkouhi, Z., Ataei, S., Esfahani, F. N., Wintrasiri, M. N., & Mozafari, M. R. (2022). Functionalized Nanostructured Bioactive Carriers: Nanoliposomes, Quantum Dots, Tocosome, and Theranostic Approach. *Curr Drug Deliv*, *19*(10), 1001-1011. https://doi.org/10.2174/1567201819666220324092933
16. Nabi, B., Rehman, S., Baboota, S., & Ali, J. (2019). Insights on Oral Drug Delivery of Lipid Nanocarriers: a Win-Win Solution for Augmenting Bioavailability of Antiretroviral Drugs. *AAPS PharmSciTech*, *20*(2), 60. https://doi.org/10.1208/s12249-018-1284-9
17. OECD. (2004). *Test No. 117: Partition Coefficient (n-octanol/water), HPLC Method*. OECD Publishing. https://doi.org/10.1787/9789264069824-en
18. Pandey, S., Jirwankar, P., Mehta, S., Pandit, S., Tripathi, P., & Patil, A. (2013). Formulation and evaluation of bilayered gastroretentable mucoadhesive patch for stomach-specific drug delivery. *Curr Drug Deliv*, *10*(4), 374-383. https://doi.org/10.2174/1567201811310040002
19. Pawar, S. D., Gawali, K., Kulhari, H., Murty, U. S., & Kumar, P. (2023). Amoxapine-Loaded Solid Lipid Nanoparticles with Superior Preclinical Pharmacokinetics for Better Brain Delivery: LC-MS/MS and GC-MS Analysis. *ACS Chem Neurosci*. https://doi.org/10.1021/acschemneuro.2c00673
20. Qian, M., Shi, H., Wang, F., You, C., Zhang, Y., & Li, X. (2025). Preparation, characterization, stability and functional properties of andrographolide loaded

kafirin/carboxymethyl cellulose composite particles using antisolvent precipitation method. *Int J Biol Macromol*, *284*(Pt 1), 138105. https://doi.org/10.1016/j.ijbiomac.2024.138105

21. Rojekar, S., Abadi, L. F., Pai, R., Prajapati, M. K., Kulkarni, S., & Vavia, P. R. (2022). Mannose-Anchored Nano-Selenium Loaded Nanostructured Lipid Carriers of Etravirine for Delivery to HIV Reservoirs. *AAPS PharmSciTech*, *23*(7), 230. https://doi.org/10.1208/s12249-022-02377-8
22. Satapathy, B. S., Kumar, L. A., Pattnaik, G., & Barik, B. (2021). Lomustine Incorporated Lipid Nanostructures Demonstrated Preferential Anticancer Properties in C6 Glioma Cell Lines with Enhanced Pharmacokinetic Profile in Mice. *Acta Chim Slov*, *68*(4), 970-982. https://doi.org/10.17344/acsi.2021.6977
23. Sharma, T., Katare, O. P., Jain, A., Jain, S., Chaudhari, D., Borges, B., & Singh, B. (2021). QbD-Steered Development of Biotin-Conjugated Nanostructured Lipid Carriers for Oral Delivery of Chrysin: Role of Surface Modification for Improving Biopharmaceutical Performance. *Colloids Surf B Biointerfaces*, *197*, 111429. https://doi.org/10.1016/j.colsurfb.2020.111429
24. Shehata, T. M., Aldhubiab, B., & Elsewedy, H. S. (2024). Virgin Coconut Oil-based Nanostructured Lipid Carrier Improves the Hypolipidemic Effect of Rosuvastatin. *Int J Nanomedicine*, *19*, 7945-7961. https://doi.org/10.2147/ijn.S463750
25. Stahl, M. A., Lüdtke, F. L., Grimaldi, R., Gigante, M. L., & Ribeiro, A. P. B. (2024). Characterization and stability of solid lipid nanoparticles produced from different fully hydrogenated oils. *Food Res Int*, *176*, 113821. https://doi.org/10.1016/j.foodres.2023.113821
26. Vishwakarma, N., Jain, A., Sharma, R., Mody, N., Vyas, S., & Vyas, S. P. (2019). Lipid-Based Nanocarriers for Lymphatic Transportation. *AAPS PharmSciTech*, *20*(2), 83. https://doi.org/10.1208/s12249-019-1293-3
27. Wani, T. U., Fazli, A. A., Raza, S. N., Khan, N. A., & Sheikh, F. A. (2022). Formulation and Pharmacokinetic Evaluation of Ethyl Cellulose/HPMC-Based Oral Expandable Sustained Release Dosage of Losartan Potassium. *AAPS PharmSciTech*, *23*(5), 160. https://doi.org/10.1208/s12249-022-02295-9
28. Xiong, F., Yao, C., Zhou, L., Li, W., Wei, B., Guan, J., & Mao, Y. (2022). [Experimental study of resveratrol-solid lipid nanoparticles in promotion of osteogenic differentiation of bone marrow mesenchymal stem cells]. *Zhongguo Xiu Fu Chong Jian Wai Ke Za Zhi*, *36*(9), 1155-1165. https://doi.org/10.7507/1002-1892.202205009
29. Yousry, C., Fahmy, R. H., Essam, T., El-Laithy, H. M., & Elkheshen, S. A. (2016). Nanoparticles as tool for enhanced ophthalmic delivery of vancomycin: a multidistrict-based microbiological study, solid lipid nanoparticles formulation and evaluation. *Drug Dev Ind Pharm*, *42*(11), 1752-1762. https://doi.org/10.3109/03639045.2016.1171335
30. Zhang, Z., Li, X., Sang, S., McClements, D. J., Chen, L., Long, J., Jiao, A., Wang, J., Jin, Z., & Qiu, C. (2022). A review of nanostructured delivery systems for the encapsulation, protection, and delivery of silymarin: An emerging nutraceutical. *Food Res Int*, *156*, 111314. https://doi.org/10.1016/j.foodres.2022.111314

